DEGREE PROJECT IN ELECTRICAL ENGINEERING,
FIRST CYCLE, 15 CREDITS
STOCKHOLM, SWEDEN 2018

A commercial vehicle's electrical startability

Elektrisk startbarhet för tunga fordon

HENRIK PERSSON

KRISTINN ARNAR ORMSSON

KTH ROYAL INSTITUTE OF TECHNOLOGY
SCHOOL OF ENGINEERING SCIENCES IN CHEMISTRY, BIOTECHNOLOGY AND HEALTH

A commercial vehicle’s electrical startability

Elektrisk startbarhet för tunga fordon

Henrik Persson
Kristinn Arnar Ormsson

Degree Project in Electrical Engineering
First cycle, 15 credits
Supervisor at KTH: Anna Josefsson
Examiner: Thomas Lind
TRITA-STH 2018:51

KTH Royal Institute of Technology
School for Engineering Sciences in Chemistry,
Biotechnology and Health
141 52 Huddinge, Sverige

This degree project was performed on behalf of
Scania AB

Abstract

In commercial vehicles, where the driver overnights with the engine turned off while still consuming electricity, it is important to know how much the battery can be discharged before reliable engine starting is at risk. The vehicle's ability to crank the engine, i.e. startability, changes with the vehicle's ambient temperature and the batteries state of charge. The aim of this project is therefore to test the startability of a commercial vehicle and its cranking system's behaviour at different ambient temperatures and battery state of charge. Physical startability tests were planned and performed on a commercial vehicle at different temperatures inside a climate chamber. The results of these tests show the torque of the vehicle's powertrain increasing with lowering temperature while the cranking system's performance decreases. This decrease in the cranking system's performance is a result of the battery's lowering ability to supply power at lower temperatures.

Keywords
Startability, commercial vehicle, cranking system, lead-acid battery, state of charge, starter motor, internal combustion engine.

Sammanfattning

I tunga fordon, där chauffören spenderar natten med avstängd motor men fortsätter att förbruka el, är det viktigt att veta hur mycket batterierna kan urladdas innan motorn inte kan startas. Fordonets förmåga att starta motorn, det vill säga dess startbarhet, ändras med omgivningstemperaturen och batteriernas laddnivå. Syftet med projektet var därför att undersöka startbarheten på ett tungt fordon samt dess startsystems beteende vid olika omgivningstemperaturer och laddningsnivåer på batterierna. Under projektets gång planerades samt genomfördes provstarter med det tunga fordonet vid olika omgivningstemperaturer i en klimatkammare. Provstarterna påvisade att släpmomentet på fordonets drivlina ökade med en fallande temperatur medan startsystemets prestanda försämrades. Startsystemets försämrade prestanda beror huvudsakligen på batteriernas försämrade förmåga att avge effekt vid lägre temperaturer.

Nyckelord
Startbarhet, tunga fordon, startsystem, blysyrabatteri, batteriladdningsgrad, startmotor, förbränningsmotor.

Acknowledgements

This degree project was performed on behalf of Scania AB and was a part of the engineering program “Högskoleingenjör i elektronik” at KTH Royal Institute of Technology. Knowledge in basic electrical theory is recommended for better understanding of the projects content.

We would like to thank Scania AB for giving us the opportunity, support and resources needed to complete this project. We would especially like to thank our supervisors:

Börje Nilsson, Scania AB
Gunnar Ledfeld, Scania AB
Anna Josefsson, KTH

Abbreviations

SoC	State of Charge
SoH	State of Health
DoD	Depth of Discharge
DC	Direct Current
Ah	Ampere hours
I	Current
A	Ampere (a unit for I)
U	Voltage
V	Volt (a unit for V)
OCV	Open-Circuit Voltage
IMR	Integrated Mechanical Relay
CCA	Cold-Crank Amps
AGM	Absorbent Glass Mat
kS/s	kilo Samples per second
CAN	Controller Area Network
rpm	revolutions per minute
IC	Internal Combustion
HD	Heavy Duty
VOR	Vehicle Off Road
PbO_2	lead dioxide
Pb	lead
H_2SO_4	sulfuric acid
SO_4	sulphate
H_2	hydrogen
$PbSO_4$	lead sulphate
H_2O	water
O	oxygen
PbCa	lead-calcium
PbSb	lead-antimony

Table of content

1 Introduction

1.1 Problem definition

In commercial vehicles, such as long haulage trucks, the driver might overnight in the vehicle and consume electrical energy from the batteries for e.g. ventilation and lighting. This consumption will, if not monitored, drain the batteries and make engine cranking impossible without recharging the batteries. Furthermore, falling ambient temperature during the night will result in decreasing battery capacity and therefore reduced battery performance (1). Knowing at what battery capacity the vehicle will start, i.e. the startability, is therefore vital to inform the driver when reliable starting of the engine is close to being threatened.

The vehicle system responsible for starting an IC , internal combustion, engine is the cranking system. Although it is quite simple in design; consisting mainly of the battery, starter motor and ignition switch, it is responsible for the reliable cranking of the engine. For reliable prediction of the vehicle's startability, it is important to understand how these components behave and how their characteristics change with the ambient environment of the vehicle. Testing of the cranking system at different ambient temperatures and battery SoC, state of charge, is therefore imperative for vehicle manufacturers to understand the vehicle's startability. Such an understanding will support further research and development of the vehicle systems and show to what extent the transient conditions, that occur at engine cranking, have on the electrical system. Additionally, it is important to study what impact cranking and discharging has on the vehicle batteries.

1.2 Goals

The aim of this project is to measure, analyse and explain the characteristic behaviours of the cranking system during engine cranking. This implies examining the vehicle startability with maximum available cranking torque at different ambient temperatures and battery SoC. Physical startability tests in predetermined temperatures are planned and performed on a commercial vehicle. Relevant physical quantities such as the current, voltage and temperature of the cranking system are recorded during the tests. The startability test's influence on the batteries will also be evaluated. Finally, the data is analysed with the help of an appropriate analytical program.

1.3 Delimitations

The focus of this project is on the cranking system at the moment of cranking. Other vehicle systems go beyond the scope of this project. A basic understanding of some of these other systems' is however vital for understanding the impact they have on the cranking system. Cranking tests are only performed on one individual engine, mounted in a commercial vehicle inside a climate chamber to simulate cranking in different environments. Pre-existing measurement systems available at Scania Södertälje are used for measurements. The tests are only performed in several predetermined temperatures, due to time limitations.

2 Theory and background

The cranking system in a commercial vehicle is designed to accelerate the IC engine to the speed required for it to be able to run independently, i.e. the turnover speed (2). The performance of the cranking system is largely determined by two factors. Firstly, by the mechanical power applied to the engine, through the starter motor, and secondly by the load that the engine puts on the starting motor, i.e. the cranking resistance (1,3). The term startability describes the cranking system's ability to reach the turnover speed desired at different battery SoC and temperatures.

Engine startability is a widely researched subject with regards to engine and fuel performance. However, the startability of a vehicle with regards to the electrical system has been researched less in the public domain. It is more common to research each component individually. The article "On Lead-Acid-Battery Resistance and Cranking-Capability Estimation" (4), however, addresses the issue of predicting a vehicle's startability. It states that a vehicle's cranking depends mainly on the available power from the battery and not from the available energy. The startability of the vehicle can therefore be estimated with the batteries' internal resistance. However, it can be difficult to measure the internal resistance as it relies on the batteries' age, SoC and temperature. In the article, a method for estimating the startability of a vehicle is proposed by measuring the batteries' resistance with a frequency-invalidation method under cranking (4).

The systems, components and characteristics important for the measurement of the cranking system's startability will be introduced and clarified in the following subchapters.

2.1 Automotive powertrain

The powertrain is the vehicle system that that generates power from an energy source, such as fuel, and delivers it to the driveline (5). It therefore provides "thrust and tractive forces required to induce motion" (6). There are many possible solutions for the powertrain systems when designing a vehicle. The vast majority of commercial vehicles have a so-called conventional powertrain, where an IC engine delivers power to the wheel through a transmission (5).

The main components of the conventional powertrain are the IC engine, the transmission, vehicle structure and system operations, see figure 1 (5). The IC engine and the transmission are of interest for this project, as they are responsible for the biggest part of the torque that the cranking system must overcome to start an IC engine (2).

Figure 1. The powertrain of a commercial vehicle (7).

2.1.1 Internal combustion engine

"Internal-combustion engines are classified as thermal engines" (6). A thermal engine is a device that compresses two mediums, often air and fossil fuel, to a specific pressure where the mixture either self-ignites or is ignited resulting in expansion of their gases (6). This expansion is then harnessed in different ways to propel diverse machines.

The primal thermal engine used in the vehicle industry is the four-stroke piston IC engine. The piston IC engine is a complex machine consisting of many moving components which generates friction when moving. Oil is used for lubricating contiguous components in the state of relative motion to reduce friction and therefore, to reduce the torque needed for the movement of the components. The oil's viscosity is however temperature dependant, it will increase at lower temperature, resulting in higher internal friction (6). The torque needed to turn the engine is therefore primarily dependent on the engines internal friction and the oil temperature along with the work needed to compress the two mediums before ignition (1).

2.1.2 Transmission

The transmission is connected to the engine. It converts the torque and speed available from the engine to the speed and load requirements of the vehicle. The torque and speed conversion are made with gears which generate friction when touching (5). Just like with the engine, a lubricating oil is used to reduce the friction and therefore the torque needed to turn the gears (6). However, it is not just the mechanical friction in the gears and the oil that contribute to the amount of torque needed to turn the transmission. It is also the transmissions design which can range from manual to fully automatic. The required torque for attaining speed is different for every design (8).

2.2 Cranking system

The cranking system's main components are the battery and the starter motor (1). The system is responsible for rotating all the masses in the powertrain until the IC engine reaches its turnover speed. The torque required to turn the powertrain is, as earlier stated, temperature dependent and increases as the

temperature decreases. The power source during cranking; the battery, is also temperature dependant and loses its ability to deliver energy in lower temperature (1). A commercial vehicle has, due to this cranking inertia, a certain minimum cranking temperature. At lower temperatures than the minimum cranking temperature, the engine will not be able to reach the turnover speed as the resistance of the driveline will have exceeded the output of the starter motor, see figure 2 (1).

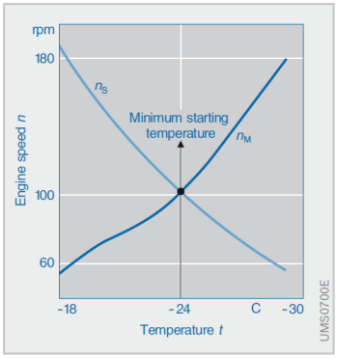

Figure 2. Diagram showing how the starter motors delivered speed curve (n_s) and the curve showing the IC engines (n_M) required speed to start, intersect at the minimum cranking temperature (1).

To better understand why the power output from the cranking system decreases with falling temperature its main component design, characteristics and limitation will be explained in the following subchapters.

2.2.1 Batteries

The starter battery works as a storage facility for electrical energy that is consumed by both the cranking system and the rest of the electrical system. This energy is delivered from the battery when the electric consumption is greater than the generated energy from the alternator (1). This usually occurs when the engine is stopped and during the cranking procedure. In commercial vehicles such as long haulage trucks, where the driver might overnight in the truck with the engine turned off, the battery has to be able to deliver energy for several hours to power appliance such as: air cooler, ventilation and lighting. These batteries must also be capable of delivering a great power for a short time during the cranking procedure. To both fulfil these requirements and remain a cost-effective storage device, the lead-acid batteries are sufficient and therefore the dominant type of battery in commercial vehicles (1).

The galvanic cell in a lead-acid battery consists of one or several positive PbO_2, lead dioxide, plates and negative-spongy Pb, lead, plates with separators between them to prevent short circuiting. The plates with the same potential within the cell are galvanically connected (9). To meet the chemical and mechanical requirements, each plate is often constructed as a grid made by PbCa, lead-calcium, alloy (10). The voids between the plates are filled with H_2SO_4, sulfuric acid, which acts as an electrolyte. The electrolyte is needed for the electrochemical reaction in the charge- and discharge procedure as well as a charge carrier for the current between the positive and negative plates within the cells (9). A fully charged cell gives a voltage of 2.12 V regardless of the size and number of parallel plates within the cell (10). Hence, six

serially connected cells give 12.72 V which is the case for a standard 12 V lead-acid battery. An example of a design for a galvanic cell is shown in figure 3.

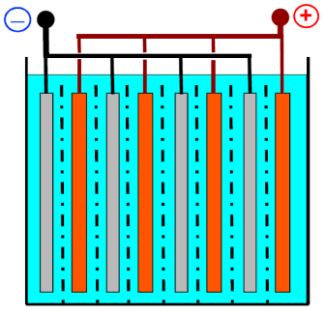

Figure 3. The connected grey plates represent the negative Pb and the copper- coloured plates are the positive PbO_2. The light blue surrounding is representing the electrolyte. The black dotted line is the separators (11).

2.2.1.1 Electrochemical reaction, lead-acid battery

A fully charged lead-acid battery consists of PbO_2 on the positive plates and Pb on the negative plates. The electrolyte consists of H_2SO_4 and H_2O, water. The density of the electrolyte is approximately 1.28 g/cm^3 in a fully charged battery and 1.10 g/cm^3 for deep discharged due to higher ratio of H_2O relative H_2SO_4 (9).

The SO_4, sulphate, breaks the chemical bond with the H_2, hydrogen, in the electrolyte during the discharging procedure and bonds with the PbO_2 at the positive plate; creating $PbSO_4$, lead sulphate. At the negative plate, the H_2SO_4 chemical decomposition will transform the Pb on the plates to $PbSO_4$ leaving free H^+ ions. These ions will bond with the left-over O, oxygen, from the positive plates and create H_2O. Hence the water ratio relative to the H_2SO_4 in the electrolyte increases. A galvanic connection between the batteries' poles causes a reaction at the negative plates that releases electrons which, due to the electromotive force, wander towards the positive plates. An electrical current therefore flows from the positive to the negative plates through the external conducting circuit. A fully discharged battery has $PbSO_4$ at both the negative and the positive plates and the electrolyte consists of H_2SO_4 highly diluted with H_2O (9). An illustration of the process can be seen below in figure 4.

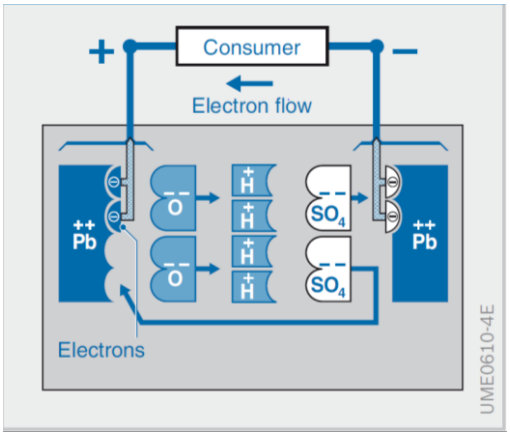

Figure 4. The electrochemical process during discharging (1).

During the recharging procedure, the reaction described above occurs reversely until the battery reaches the state of fully charged as described earlier. If a fully charged battery gets overcharged, H_2 and O in gas forms are generated i.e. gassing. The battery loses weight during gassing as the water is consumed. The total reaction for charging and discharging can be seen in formula 1 (9).

$$Pb + PbO_2 + 2H_2SO_4 \Leftrightarrow 2PbSO_4 + 2H_2O \quad [1]$$

2.2.1.2 Lead-acid battery design

Low-maintenance or maintenance-free batteries with a low water consumption (less than 4 g /Ah), are the most common lead-acid battery types in vehicles. They have longer maintenance intervals than conventional ventilated batteries (1). These long intervals are achieved by creating the plates of alloys e.g. PbCa at the negative plates and an PbSb, lead-antimony, at the positive plates. The electrochemical characteristics of the alloys increase the voltage where gassing occurs and decrease self-discharge. The higher gassing voltage decreases the water consumption and makes the battery more resistant for overcharging (8).

The design of the plates in the battery and the number of them are significant for the cranking capacity and the cycling performance. With an increase in plate numbers, the plates get thinner and the plate surface-area increases in the battery. This increased surface area enables the battery to deliver the high power required during cranking and decreases the battery's weight. This leaves the battery, however, more sensitive to vibrations and reduces its cyclic lifetime (12). Figure 5 shows a correlation of the plates design and quantity. A compromise of the number of plate and their thickness is required to fulfil the requirements present in many commercial vehicles, such as several electrical consumers, vibrations and high cranking torque. The often-named HD, heavy duty, battery fulfils these requirements by combining these designs aspects to make the battery maintenance free, deep-cycle resistant and vibration proof. Due to its large size, the HD battery is also capable of delivering sufficient cranking power (1).

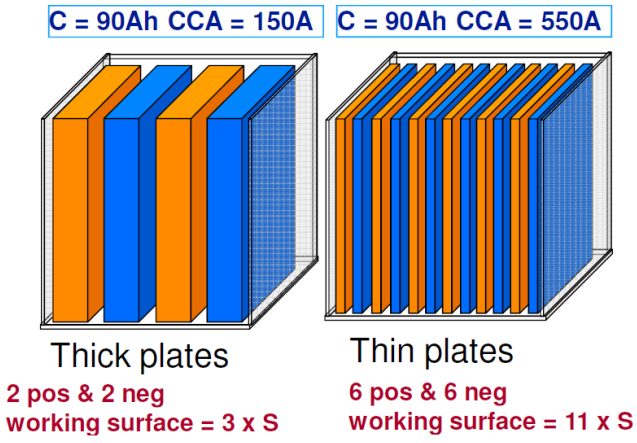

Figure 5. The different battery characteristics between few thick plates and several thin plates. C is the maximum available capacity and CCA is the cold-cranking current (11).

Other designs of lead-acid batteries are e.g. gel-batteries and AGM, absorbent glass mat, batteries. The gel-battery have a silicon compound in the electrolyte to make it jelly-like. It is supreme for deep-cycling and is completely maintenance free (1,10). AGM batteries the electrolyte bound in fibreglass mats. This results in a low internal resistance and makes the battery suitable for engine cranking and deep-cycling (10).

2.2.1.3 Characteristic and behaviour

The battery's capacity to deliver electrical energy in a specified condition is measured in Ah, Ampere hours (1). The amount of available capacity is known as the SoC, state of charge, and is defined as the quotient of the actual amount of charge and the maximum possible amount of charge, see equation 2 (13).

$$\mathrm{SoC} = \frac{\text{amount of available capacity}}{\text{maximum possible amount of charge}} \qquad [2]$$

DoD, depth of discharge, is defined as 1-SoC and presents the amount of consumed energy from the battery (13). The SoC is evaluated by different methods e.g. open-circuit voltage, electrolyte-density control or by measuring the discharging current over a certain time.

OCV, open-circuit voltage, is measured over an unloaded battery i.e. open circuit. From the instant when the battery has been set in open-circuit state after charging or discharging, it will take some time, even days before it reaches a steady-state voltage. To compute the SoC with accuracy through OCV, the battery has to reach the steady-state voltage (1). This method is therefore less suitable for operations where the open-circuit time is short or if the battery never gets unloaded.

Evaluation of the SoC by measuring the density of the electrolyte is a common method. It's achieved by placing a sample of the electrolyte in a hydrometer which gives the relative density of the liquid. The relative density is then converted into SoC (9). Due to the corrosive nature of the acid, this method may be hazardous.

Yet another method is, as mentioned earlier, obtained by measuring the current during the discharge of the battery. By measuring the current drawn from the battery over a certain time, the summed drawn energy can be computed (in Ah). To compute the SoC with this method, the SoC has to be known when the discharging procedure starts. The relationship between the discharging current strength and the drawn capacity in Ah is however nonlinear. Hence considerations for the current strength must be taken to get an accurate result (1). The nonlinear behaviour follows Peukerts equation which states that the total amount of capacity decreases as the discharging current increases. This is shown in equation 3 where C_{n1} is the actual available capacity at the discharging current I_{n1} and C_n is the available capacity at the current I_n. pc is the Peukert coefficient which normally is between 1 and 1.47 in lead-acid batteries (14).

$$C_{n1} = C_n \left(\frac{I_n}{I_{n1}}\right)^{pc-1} \qquad [3]$$

This nonlinearity is caused by an increasing internal resistance between the electrolyte and the active material at the positive plates when the discharging current increase. The recovery rate of the active material at the positive plates is also affected and decreases while the current increases. This is caused by a reduced number of active centres, that can react with the electrolyte, at the positive plate (15). The accuracy of Peukerts equation is dependent of a constant temperature and current. An accurate implantation of this equation is therefore difficult to implement outside of laboratory environments with steady conditions. (15).

The available capacity follows the battery's temperature. When the temperature drops, the SoC decreases due to higher viscosity of the electrolyte which slows down the electrochemical process and makes it less efficient. Higher viscosity also increases the internal resistance. The capability to deliver high power during cranking is therefore reduced at lower temperatures (1).

Due to the lead-acid batteries SoC correlations to temperature and discharging current strength, the nominal capacity is stated by the standard EN 50342. EN 50342 describes different standardized cases where the battery is discharged with a constant current for a fixed time at +25 C°. For example, a 12 V battery that is specified with the capacity 44 Ah at C20 discharge, can be discharged with the constant current 2,2 A (44 Ah/20 h) for as a minimum 20 hours before it reach the deep-discharged voltage 10.5 V at +25 C° (1). Table 1 shows the available capacity for a Scania super HD c-type battery at different temperatures and with different standardized discharging rates, given by the battery manufacturer.

Table 1. The guaranteed capacity of a 230 Ah Scania super HD c-type battery at different conditions.

Temperature[C]	current [A]	capacity [Ah]	rate
25	56,25	180	C4
	22,50	209	C10
	11,25	220	C20
	2,25	247	C100
0	56,25	143	C4
	22,50	165	C10
	11,25	166	C20
	2,25	206	C100
-10	56,25	112	C4
	22,50	135	C10
	11,25	140	C20
	2,25	155	C100
-20	56,25	94	C4
	22,50	107	C10
	11,25	115	C20
	2,25	133	C100

As the electrochemical process slows down with lowering temperature, so will the battery's capability to deliver high output power at low temperatures. The standard EN 50342 specifies a CCA, cold-crank amps, test which is performed with a specified cranking current at -18 C° for 10 seconds. After the first 10 seconds, the

voltage may not drop below 7.5 V. Afterwards, the battery will rest for another 10 seconds before it gets discharged by 60% of the CCA current for 73 seconds. Directly after the last discharge, the voltage may not fall below 6 V (9). The CCA may be specified by other standards such as SAE where the battery gets discharged with the cranking current in 30 seconds. Then the afterward voltage must be over 7.2 V (9).

All these earlier described behaviours of the lead-acid battery are not forever constant. The batteries age by e.g. cycling, deep discharging (<10.5 V for 12 V batteries), corrosion, overcharging and sulphating (16). Sulphating occurs at the negative- and the positive plates when the SoC is below 65%. If the sulphating goes on for too long, the battery may never be able to get recharged (17). The degradation of the batteries is measured as the SoH, state of health. The SoH is defined as the battery's current condition compared with its ideal conditions (when it is new). It can be measured by several parameters such as internal resistance, frequency response or capacity (13).

2.2.1.4 Charging

Charging of the batteries in a vehicle is normally performed by an alternator which produces a voltage between 13,5-15 V for each 12V battery. The alternators varying voltage range is due to the ambient temperature's effect on the battery's gassing voltage (1). The voltage increases by 0.3 V for every 10°C the battery temperature drops.

Charging the battery as close as possible to the gassing voltage is important to avoid over- or under-charging which can harm the battery's health i.e. SoH (18). Charging while the engine is turned off is obtained by a separate battery charger. Modern battery chargers use switching technologies to adjust the charging voltage very precisely. They have different charging modes for different types of batteries. The charging procedure can be by described by with the following three phases: (18).

Phase 1 : The battery is charged with the maximum current that the charger can deliver until the gassing voltage is reached. Approximately 90% of the battery's SoC is reached during this phase.
Phase 2 : The charger keeps the voltage constant close to the relevant gassing voltage at the current ambient temperature.
Phase 3 : The battery gets a little bit overcharged in order to generate gassing. The gassing is necessary for stirring the electrolyte, which gets stratified due to the different density of the acid and the water. After that phase, the battery gets some maintenance charge to prevent self-discharging.

2.2.2 Starter motor

An IC engine needs assistance to achieve the momentum needed for it to start and run independently (2). The resistance of the engine's exhaust, induction and the compression strokes must be overcome. Additionally, the bearings of the engine are not properly lubricated at the starting instance resulting in high friction. In commercial vehicles, a starter motor is used to generate the large forces needed to

crank it (2). Figure 6 shows a cross section of a starter motor with component description.

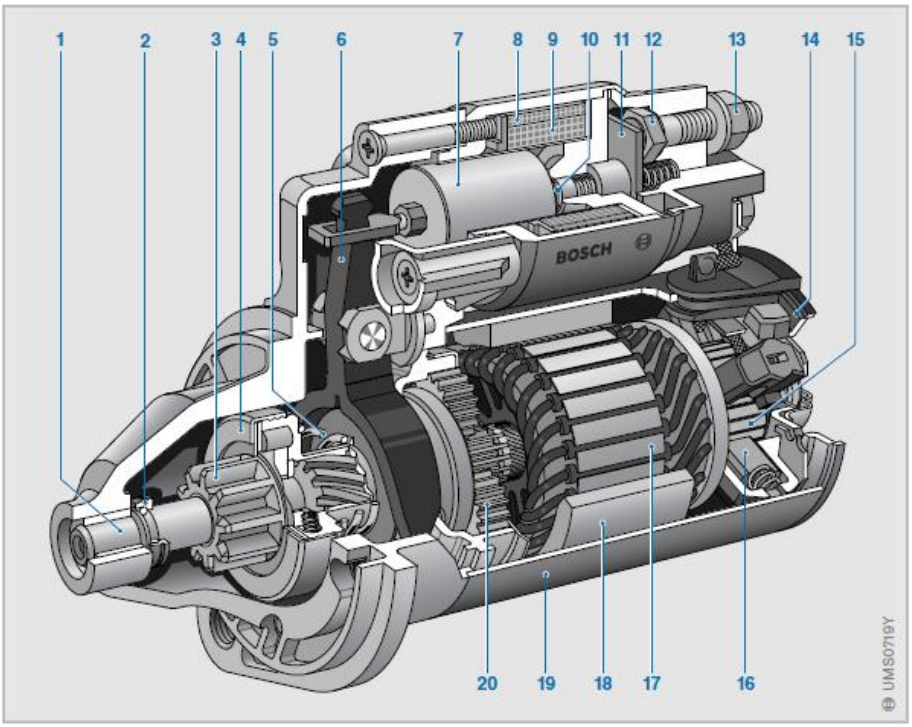

Fig. 6
1 Drive shaft
2 Stop ring
3 Pinion
4 Roller-type overrunning clutch
5 Meshing spring
6 Pinion-engaging lever
7 Solenoid switch
8 Hold-in winding
9 Pull-in winding
10 Return spring
11 Switch contact
12 Switch contact
13 Electrical connection
14 Commutator end shield
15 Commutator
16 Brush holder
17 Armature
18 Magnet
19 Stator housing
20 Planetary gear

Figure 6. Starter motor for a commercial vehicle (2).

2.2.2.1 Serial-wound DC motor

The energy required to start an IC engine is usually drawn from the vehicle battery (1). Therefore, it is quite common to use a DC, direct current, electric motor as a starter motor. The series-wound DC motor is particularly well suited for the task (1). It delivers high torque at low speeds for overcoming the static friction within the IC engine at the moment of cranking. As the torque decreases the angular velocity of the motor increases, enabling the engine to reach the desired turnover speed (2). Today, most commercial vehicles are equipped with series-wound DC motor for cranking (2).

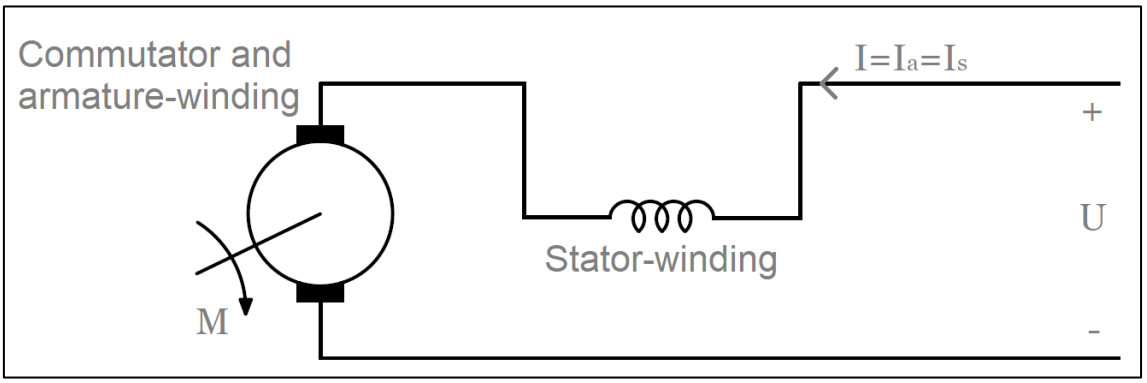

Figure 7. A equivalent circuit schematic of a series-wound starter motor.

The series-wound DC motor has the stator-winding connected in a series with the armature-winding (19). Therefore, the same current runs through the armature winding (I_a) and the stator-winding (I_s) as seen in figure 7 (19). The stators magnetic field is created electromagnetically by the stators excitation-winding which is wound round the pole shoes, as seen in figure 8 (2).

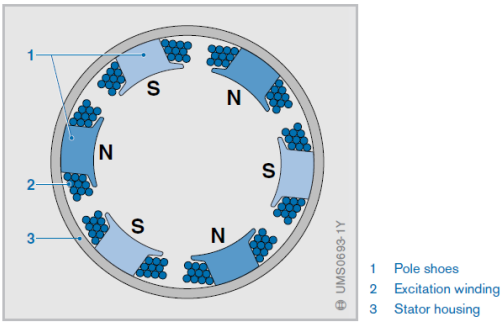

Figure 8. A series-wound motors stator housing (2).

The torque, M, in a series-wound motor is, as for other DC motors, proportional to the current, I, and the magnetic induction, B, of the magnetic field. Other factors have effect on the torque, but they are constant for every motor and can be approximated to machine constants, c (2). Equation 4 shows the torque formula.

$$M = c \cdot B \cdot I \qquad [4]$$

However, the earlier mentioned series-connection gives the motor some distinctive characteristics. One is that the magnetic induction, B, is current dependant, as seen in equation 5 (2). With these characteristics, a new torque formula for the series-wound DC motor can be expressed where the torque increases quadratically relative to the current and another machine constant, c_1, as seen in equation 6 (19).

$$B = c_1 \cdot I \qquad [5]$$

$$M = c \cdot c_1 \cdot I^2 \qquad [6]$$

This is thought, only true for low currents since the iron in the pole shoes will saturate at higher currents, meaning that the magnetic induction will cease to increase proportionally (2). The motor torque will consequently stop increasing quadratically and start to increase proportionally to the current as the magnetic induction will have become a constant, $\hat{B}$, (2), see equation 7.

$$M = c \cdot \hat{B} \cdot I \qquad [7]$$

Another characteristic of the series-wound motor is the rotation speed, n. Equation 8 shows how the power output, P, of the motor is given by the product of its angular velocity, ω, and torque (2). Rewriting of equation 8 shows that the rotation speed is inversely proportional to the torque and the magnetic induction. By replacing the torque with equation 4, it can furthermore be shown that the rotation speed of the motor is inversely proportional to the current, as seen in equation 9.

$$P = \omega \cdot M = 2 \cdot \pi \cdot n \cdot M \quad [8]$$

$$n = \frac{P}{2 \cdot \pi \cdot M} = \frac{P}{2 \cdot \pi \cdot c \cdot B \cdot I} \quad [9]$$

Equation 10 shows that the power output, P, of the series motor is proportionate to its power input, P_i, and the starter motor's efficiency, μ (19). A new rotation speed equation can therefore be attained as the power input is proportionate to the input voltage and input current. Inserting equation 10 to equation 9 gives a new motor speed equation 11, which shows that the series-wound motors speed is proportional to its input voltage.

$$P = \mu \cdot P_i = \mu \cdot U \cdot I \quad [10]$$

$$n = \frac{\mu \cdot P}{2 \cdot \pi \cdot c \cdot B \cdot I} = \frac{\mu \cdot U}{2 \cdot \pi \cdot c \cdot B} \quad [11]$$

Figure 9 shows a schematic of a series-wound starter motors characteristics as a function of the current. It shows how the torque rises quadratically at lower current levels and how it gets proportional at higher current levels. It also shows how the rotational speed decreases hyperbolically with higher current and therefore higher torque. Finally, it shows how the voltage follows the motors rotational speed. The current in figure 9 starts at around 150A as a certain minimum current is needed to turn the motor (2).

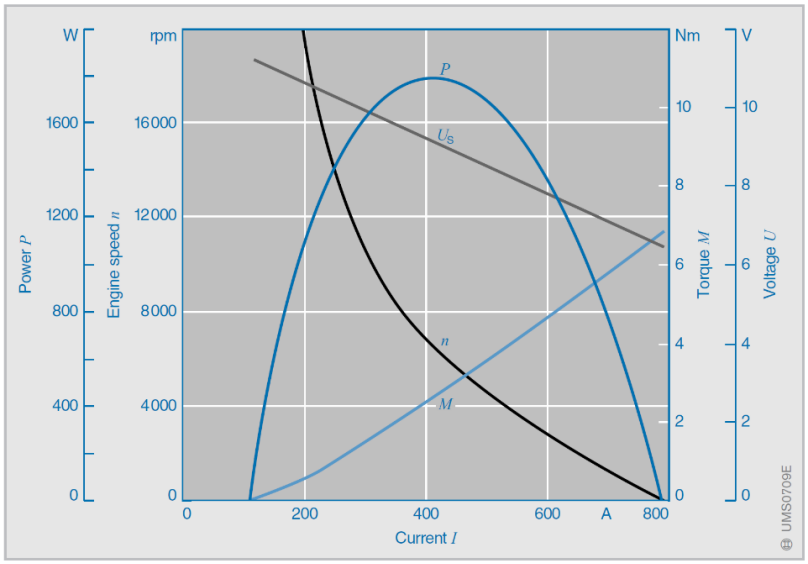

Figure 9. A schematic diagram of a serial-wound starter motors characteristics (2).

2.2.2.2 The cranking mechanism

The torque conversion from the starter motor to the IC engines ring gear, which turns the engine, happens by way of a small gear called a pinion (1). But as this torque is only needed for the cranking of the IC engine, and not for when its running independently or has stopped, the starter motor is equipped with a pre-engage drive

for meshing the pinion and the ring gear together for cranking (1). A commercial vehicle's starter motor uses a two-stage pinion-engagement sequence for starting the IC engine (2). The first stage guarantees the successful meshing of the pinion to the ring gear and the second one turns the starter motor until the engine runs independently.

The first stage begins when the ignition key is turned and the ignition switch closes. The switch delivers a voltage signal to an IMR, integrated mechanical relay, pre-control relay, which switches the high current required for the cranking of the two-stage system (2). The current from the batteries, then flows through the IMRs contacts to the solenoid switch. When the solenoid switch is energized, it generates a magnetic field and starts pulling the pinion engaging-lever, which in turn pushes the pinion and the overrunning clutch towards the ring gear. In the first stage, the solenoid is connected in parallel to the motor through a series resistance. This insures that sufficient current flows through the series resistance to the commutator and the stator. The current holds the armature fixed or rotates it is slowly for higher probability of meshing (2).

The second stage begins just before the pinion is fully meshed. Then the solenoid switch changes position and disconnects the parallel connection through the series resistance to the armature (2). Immediately after that, the pinion will reach its final position (fully meshed) and the solenoid switch connects the series-motor directly to the batteries, i.e. the main circuit closes (2). Enabling it to "generate its full torque output" (2).

When the IC engine starts to run independently and rotates quicker than the starter motor, then the overrunning clutch disengages the pinion from the pinion drive shaft. By doing so, it protects the armature of the series-motor from accelerating to excessive speeds (2). When the engine is running independently, the ignition key is released, which opens the ignition switch (2). Then the solenoid switch loses its magnetization current and the pinion travels back to its original position, with the help of the return spring, and opens the main circuit (2). Figure 10 shows the cranking systems circuit with component description.

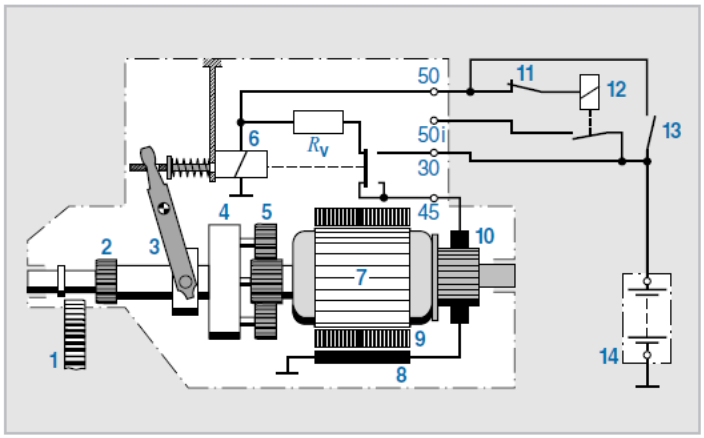

Figure 10. Schematic of the serial-wound starter motor for commercial vehicles with an electrically operated two-stage engaging mechanism (2).

2.3 Digital measurement systems

Measuring physical quantities like voltage, electric current and temperature can either be performed analogously or digitally. Digital values are gathered by sampling an analogue signal which is then quantified and converted into digital values (20). The sample rate is an important parameter and according to Nyquist's theorem, the sampling rate must at least double the highest frequency of the sampled analogue signal. Otherwise some of the signal's information will be lost. The sample rate is therefore often much higher than the frequency of the sampled signal in order to get higher resolution. (20). Figure 11 shows the result of different sampling rates.

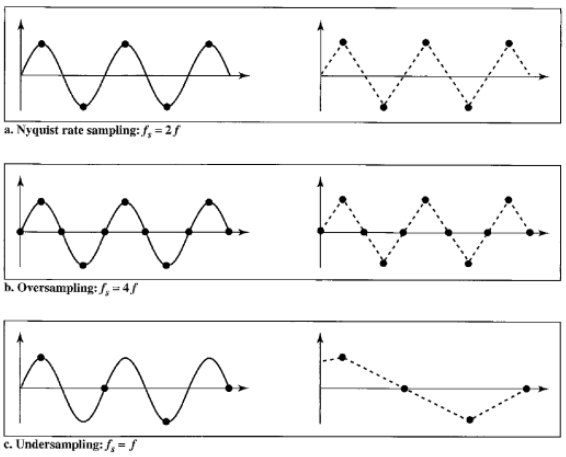

Figure 11. Shows a signal with different sample rate (20).

All electrical signals have thermal- and induced noise (20). The signal's noise is therefore included when the signal is measured. Furthermore, the measurement instrument's internal noise will distort the measured data even more (21). By adding an analogue or digital lowpass filter, the noise can be reduced. The digital filter is a numerical operation that process the recorded data mathematically. An advantage with the digital filter is that it can be applied on the recorded data after the measurement is completed (21).

2.3.1 Shunt resistor

Electric current is a flow of free electrons, travelling in the same direction through a conductor (22). Ohm's law, equation 12, states that a current running through a resistive material is directly proportional to the electric potential difference, i.e. voltage, over the resistances (6,22).

$$\mathrm{I} = \frac{\varphi(P_2) - \varphi(P_1)}{R} = \frac{U}{R} \qquad [12]$$

A current running through a circuit can be calculated by measuring the voltage over a conductor with a known resistance, connected in series with the load. This kind of a current measurement device is called a shunt resistor ammeter, see figure 12.

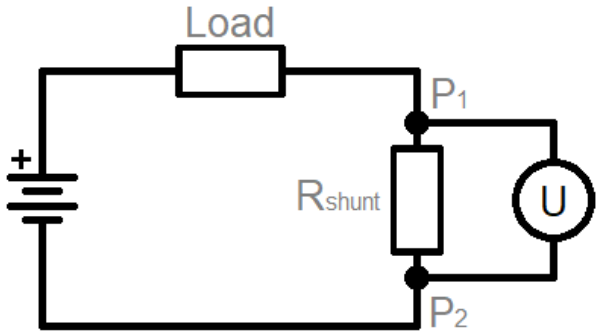

Figure 12. Schematic showing a circuit with a shunt-resistor connected to it for current measurement.

The current, i.e. electron flow, will however heat up the conductor because of internal friction and collision of the electrons in the material. Conductors have a positive temperature coefficient, meaning that an increase in heat will increase the internal friction and collision of the electrons. Which in turn increases the resistance. Equation 13, states that the conductor's resistances, R(T) is proportional to its temperature, T, and that the rate of change is dependent on the conductor's temperature coefficient, T_{ref} (22).

$$R(T) = R(T_{ref}) \cdot [1 + \alpha(T - T_{ref})] \qquad [13]$$

It is therefore important, for an accurate current measurement over a wide current range, that the shunt resistor is constructed from a material with low temperature coefficient.

2.3.2 Temperature measurements

One of the most commonly measured physical quantity is temperature (23). It can be measured electronically with many different types of sensors. Thermocouples are classical and widely used sensor for measuring temperature (24).

Thermocouple temperature-sensors utilize the Seebeck effect. It states that "thermoelectric voltage is produced and an electric current flows through a closed circuit of two dissimilar metals if the two junctions are held at different temperatures" (24). The current is proportional to the temperature difference between the two junctions and the types of metals used. Making it possible to measure the temperature difference between the two junctions by placing a voltage measuring devices in the circuit (24).

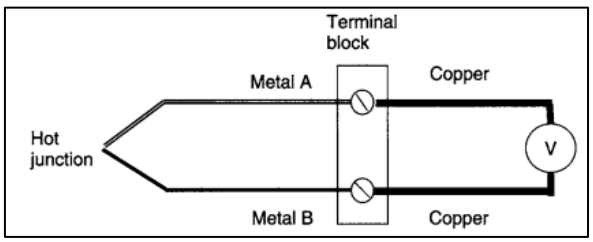

Figure 13. A descriptive figure of a thermocouple sensor (11).

The temperature of one of the junctions must be known as a reference for precise temperature-measurement. This reference junction is called the cold junction while the other junction, that is place in the measurement area is called the hot junction (24,23). The term cold junction, historically derives from the practice of placing the reference junction in an ice bath to maintain a constant 0°C for reference. The reference temperature can also be performed by tracking the cold junction temperature with the help of a compensation circuit that as seen in figure 14 (23).

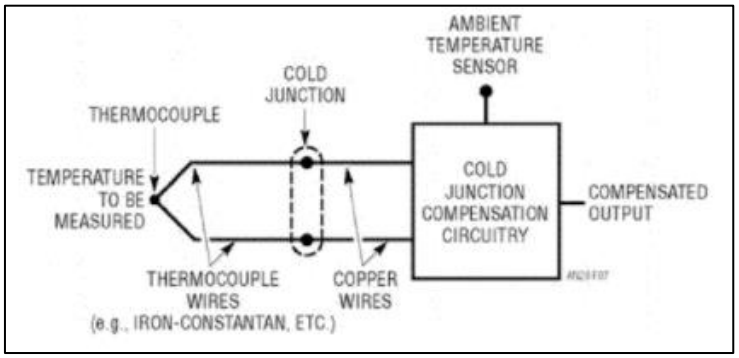

Figure 14. A thermocouple sensor with cold junction compensation circuit (23).

Thermocouple sensors have a wide temperature measurement range from -270°C to +2600°C depending on the two metals. They are therefore well suited for measuring very low and very high temperature with a typical accuracy of ±1° (24).

3 Method

For this project, the startability was measured on a long haulage truck provided by Scania. The vehicle had a 13-litre inline six-cylinder 450 horsepower engine, connected to an opticruise transmission. A series-wound Bosch starter motor with a 5.5 kW effect was mounted to the engine. The starter motor was connected to two series connected 12V Scania Super HD batteries specified with a 230 Ah capacity (at C20) and a 1200A CCA. The vehicle was refuelled with winter diesel before the startability test where performed, to prevent clogging in the fuel system due to paraffin formation at lower temperatures.

The vehicle was placed inside a climate chamber to measure the startability at different but stable ambient temperatures. The climate chamber that was used could generate temperatures between +40 to -34˚C. Startability test were performed on the vehicle under a 3-week period. During that time, several temperatures where measured and analysed.

3.1 The test procedure

The startability tests where the same, with regards to the procedure, for each temperature. Firstly, the batteries were charged up and the climate chamber set to the desired temperature. When the batteries were at full capacity and the temperature was at the desired level, were the startability test for that temperature be performed. The startability test, for each temperature, involved a number of starts with a discharging phase in-between each start until the engine could not start anymore. A last discharging phase followed the last, and failed, attempted start for each temperate. In this last phase, the batteries were discharged until one of them dropped below the deep discharge voltage (10.5V). Then the batteries were charged again, with one or two CTEK chargers, and the temperature in the climate chamber set to the next desired temperature.

The desired condition of the engine at the time of each crank, was for it to have as high a torque as possible. That was achieved by cranking the engine for as short a time as possible and therefore minimising the lubrication of the engine and transmission. When cranking, the ignition key was therefore immediately turned off as soon as the engine began run independently and the engine consequently stopped. By doing so, the spreading of oil inside the engine and transmission could be held at minimum during each engine start. This cranking method was used to imitate the condition of the powertrain during a typical cold start, i.e. when the engine temperature matches the ambient temperature.

The current of the discharging phase was decided to be 11.5A, equivalent to the battery's C20 current. The discharging circuit consisted of two parallel connected constant current loads and a timer relay. The time of each discharging phase, i.e. time between each starting attempt, was decided to be 2 hours in the beginning of each temperature. This 2-hour interval was selected to allow the oil, that had spread around the engine and transmission during cranking, to run back down to the engine's sump. The time interval was however shortened, to 1 hour or 30 minutes, as

the batteries' capacity decreased. This was done to get a better understanding of at what SoC the vehicle could not start for each temperature.

The vehicle's batteries were swapped out for a new set of identical batteries, before the startability tests began. That was done as the SoH of the vehicle's old batteries was unknown. A standardised C20 test, in accordance with EN 50342-1:2006, was performed on the new batteries before they were placed in the vehicle's battery box. An identical C20 test was then performed on the batteries after the startability tests on the vehicle where done to see how the tests had affected the batteries, i.e. SoH.

3.2 Measurement circuit

Measurement of the cranking circuit's current and voltage during cranking was of main concern for this project, as the focus was on the cranking system's performance. The voltage over each of the circuit's components along with the vehicles ground was measured to get an overview of the circuit's total voltage drop. The circuit's current was also measured along with the temperature of both batteries and the engine. The temperature was measured to see how the temperature, especially the batteries' temperature, changed with every cranking of the engine and discharging phase.

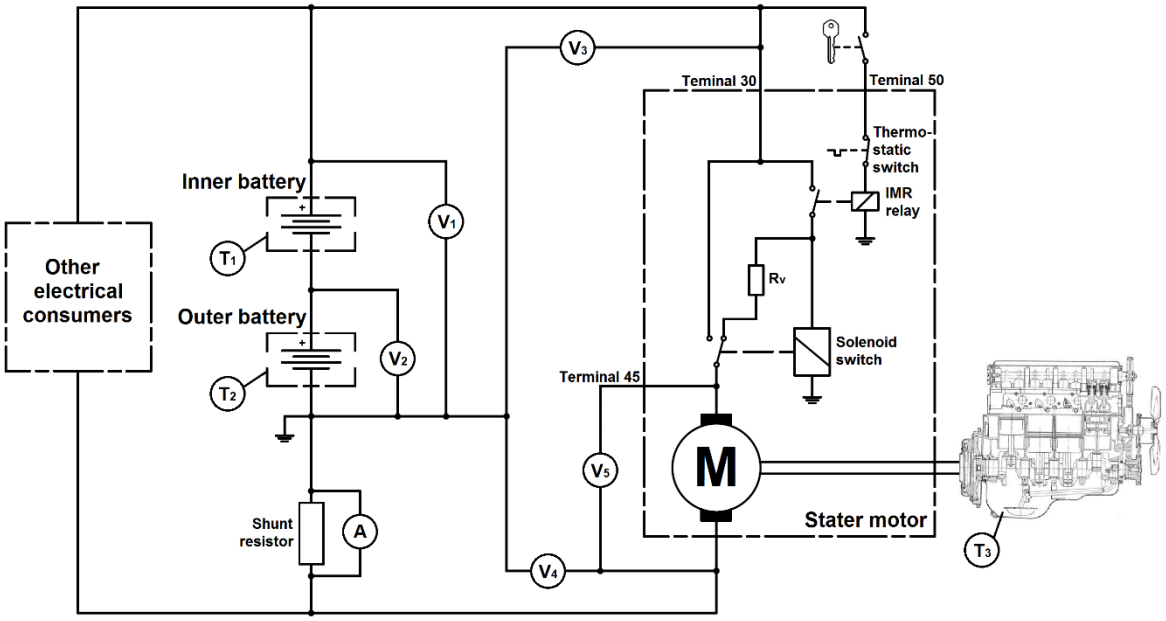

Figure 15. Schematic of the cranking system with all measuring points.

Figure 15 shows a circuit diagram of the cranking system's electrical circuit with the measurement points. The battery that sat nearer to the vehicles chassis was defined as the inner battery and the other as the outer battery. The outer battery's negative pole was defined as the circuit's ground and consequently the voltage measurement reference point. The outer battery, therefore, had a 0V to 12V voltage over it while the inner battery had a 12V to 24V voltage over it.

V1 measured the voltage over both batteries while V_2 only measured the voltage over the vehicles outer battery. V_3 measured the voltage over the starter motor's whole circuit and the vehicles ground, while V_4 only measured over the vehicle ground. By

then subtracting V_2 from V_1 could the voltage over the inner battery be obtained. Similarly, the voltage over the starter motor could be obtained by subtracting V_4 from V_3. The last voltage measurement, V_5, was from the starter motor's terminal 45 to its circuits connection to ground, i.e. only over the armature and shunt winding of the starter motor.

Coaxial cables where used for voltage measurements. The coaxial measurement cables were connected in two different ways depending on the length from the measurement device to the measurement point. When the measurement point was less than 1 meter from the measurement device, both the inner core and the outer shield were used to convey measurement signals, see method 1 in figure 16. However, when the measurement distance was longer than 1 meter, the coaxial cables shield wire was connected to ground and only the inner core of the coaxial cable was used to convey measurement signals, see method 2 in figure 16. This was done as the shield wire could work as an antenna, i.e. add unwanted noise to the measurement signal, when the coaxial cable lengthened. By connecting the shield wire to the vehicles ground, the noise added would not distort the measured signal.

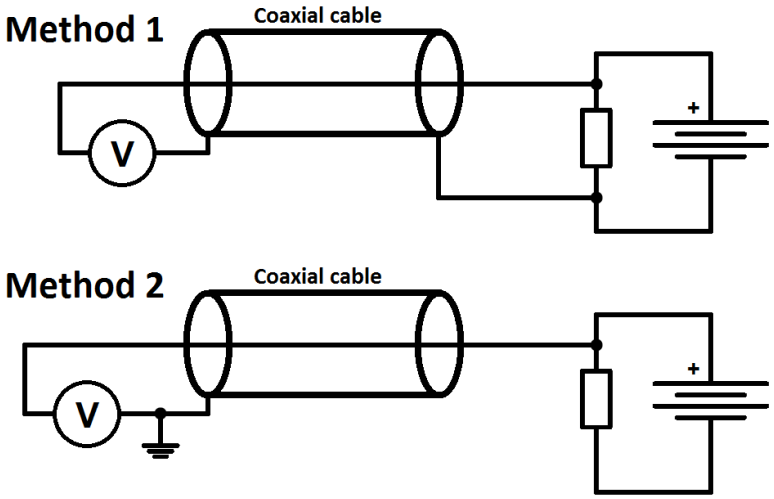

Figure 16. The two different voltage measurement methods used.

A test of the two methods on the cranking system was performed to verify the difference between the methods. It showed that the voltage difference was small, (method 2 gave a ca. 15mV higher voltage rate than method 1) and that no noticeable noise difference was between the signals, see figure 17. It was decided to use method 2 for measurement of both V_3 and V_4 as they were the furthest apart from the measurement device and the coaxial cables were already installed according to method 2 after the test between the methods. All other voltage measurements were measured with method 1.

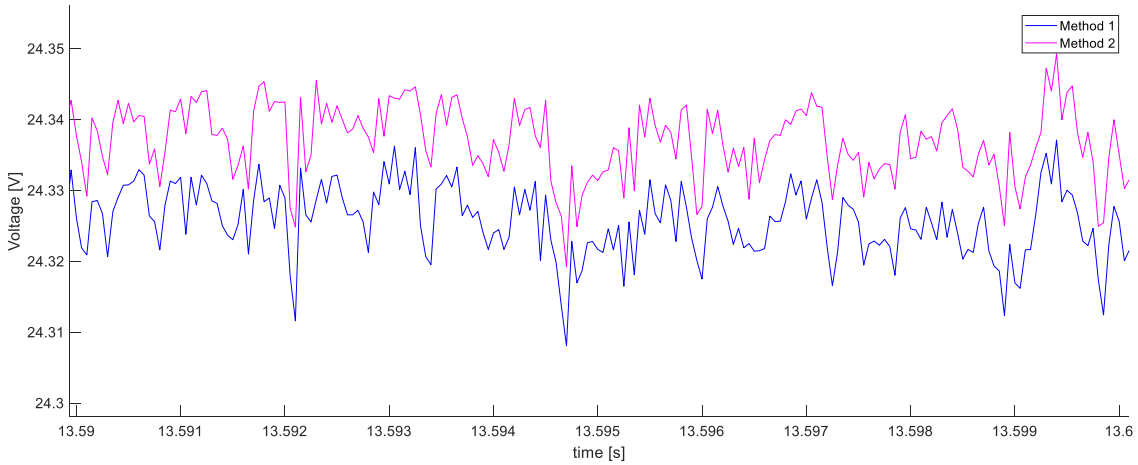

Figure 17. The difference between voltage method 1 and 2.

A shunt resistor ammeter was used for the cranking circuit's current measurement. It was connected in series with the outer battery's negative pole as seen in the figure 15. The shunt resistor's conducting material, which was measured over, was made from the alloy Manganin with the resistance 0.1mΩ. Manganin has an extremely low temperature coefficient, only 10μ K^{-1} (25), which meant that its resistance would stay almost the same in a wide range of temperatures. The shunt resistor's accuracy did therefore not change with the change in temperature. Figure 18 shows the resistance change of Manganin compared with copper which has a temperate coefficient of around 0.004 K^{-1} (26).

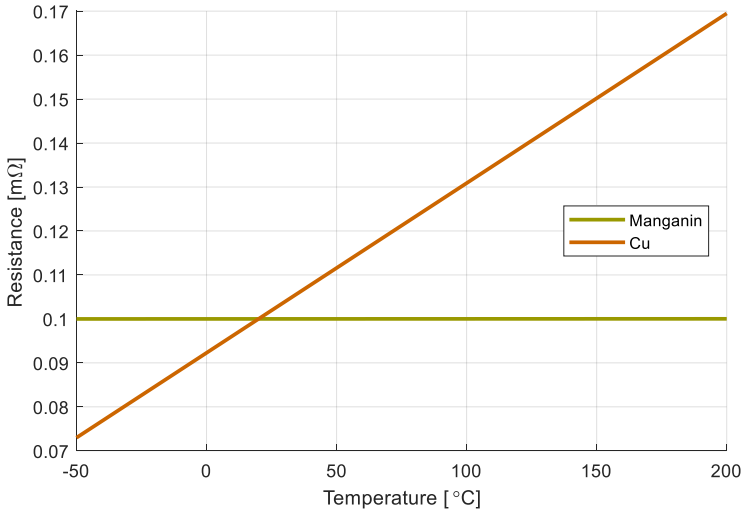

Figure 18. The resistance of Manganin and copper at different temperatures.

The shunt resistor ammeter that was used was not calibrated, it was just a resistor with a fixed resistance. The sampling rate of this analogous shunt resistor was therefore only limited to the sampling rate of the measurement device it was connected to. Other calibrated digital shunt resistor ammeters were available, but they had a limited sampling rate of maximum 1.5 kS/s, kilo samples per second. This

sampling rate was deemed too low, as will be explained in the chapter measurement devices, and therefore could not be used.

The analogue shunt resistors accuracy was measured by comparing it to a calibrated digital shunt resistor. The test showed that the analogue shunt was quicker to measure but had a 1 A to 4 A higher current rating then the digital shunt. This measurement difference resulted in a big proportionate difference between the two shunts at lower current levels, whereas at higher current levels the proportionate difference was small. The analogue shunt was therefore used as it was deemed sufficiently accurate and gave a measurement with the desired sampling rate. Figure 19 show the results from the shunt resistors test.

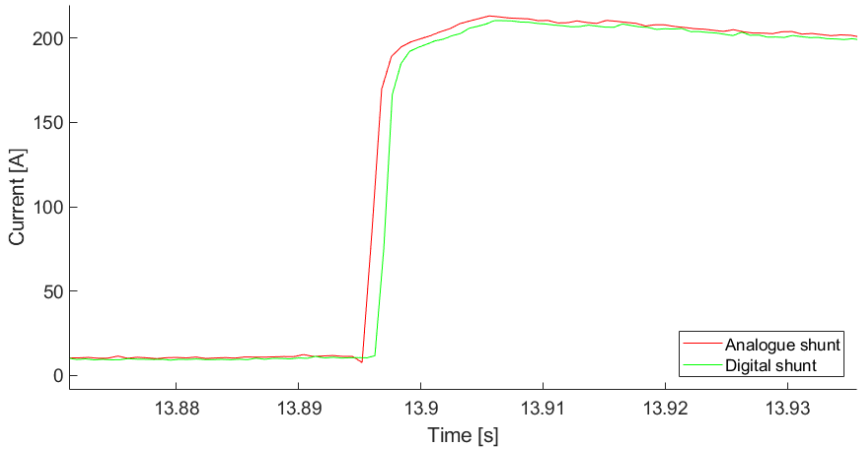

Figure 19. The difference between the digital- and the analogue shunts.

Thermocouple sensors were used to get a sense of how the temperature of the batteries changed during the startability tests and the discharging phases. The thermocouple sensors were well suited as they were small, flexible and could easily be mounted on the batteries. One sensor was mounted on each. The engines oil temperature was also measured to see if the engine had reached the desired temperature before the startability tests were performed. A preinstalled PT100 temperature sensor that measured the engine's oil sump was used to for the oil temperature measurement.

3.3 Measurement devices

A widely used signal carrying system in vehicles and in vehicle development is the so-called CAN, controller area network (1). The CAN voltage- and current measurement devices available during the course of the project had a maximum sampling frequency of 1.5kS/s. The transient conditions, in the cranking system when cranking, were however very fast and a quicker measurement system was needed to measure the fastest transients with better accuracy.

The measurement device that was used for measurement of the cranking circuits current, voltages and oil temperature was DEWE 43 A from the company DEWEsoft. It was small, powerful and versatile. The DEWE 43 A was capable of measuring eight analogue inputs simultaneously, each with a sample rate of up to 200 kS/s and a

voltage range of ±10V. Additionally it had two isolated, high-speed CAN-bus channels, a mini USB connection and power cables. The DEWE 43 A had to be connected to a computer to set up the measurement settings, as it did not have a screen. The software used for the set up was DEWEsoft's own X2 program (27).

DEWEsoft's DSI and ADAP adapters were mounted to the RS232 ports of the analogue inputs to easily connect different types of sensors to the DEWE 43 A. The adapters MSI-BR-V-200 was used for when the input voltage was higher than 10V, such as when measuring the battery and starter motor voltage. ADAP-D9M-LEM2 in connection to a LEMO to BNC converter to measure up to 10V signals, such as the shunt resistor and battery ground, with a coaxial cable. MSI-BR-RTD-L adapter was then used to measure the engine's oil temperature with the earlier mentioned PT100 sensor.

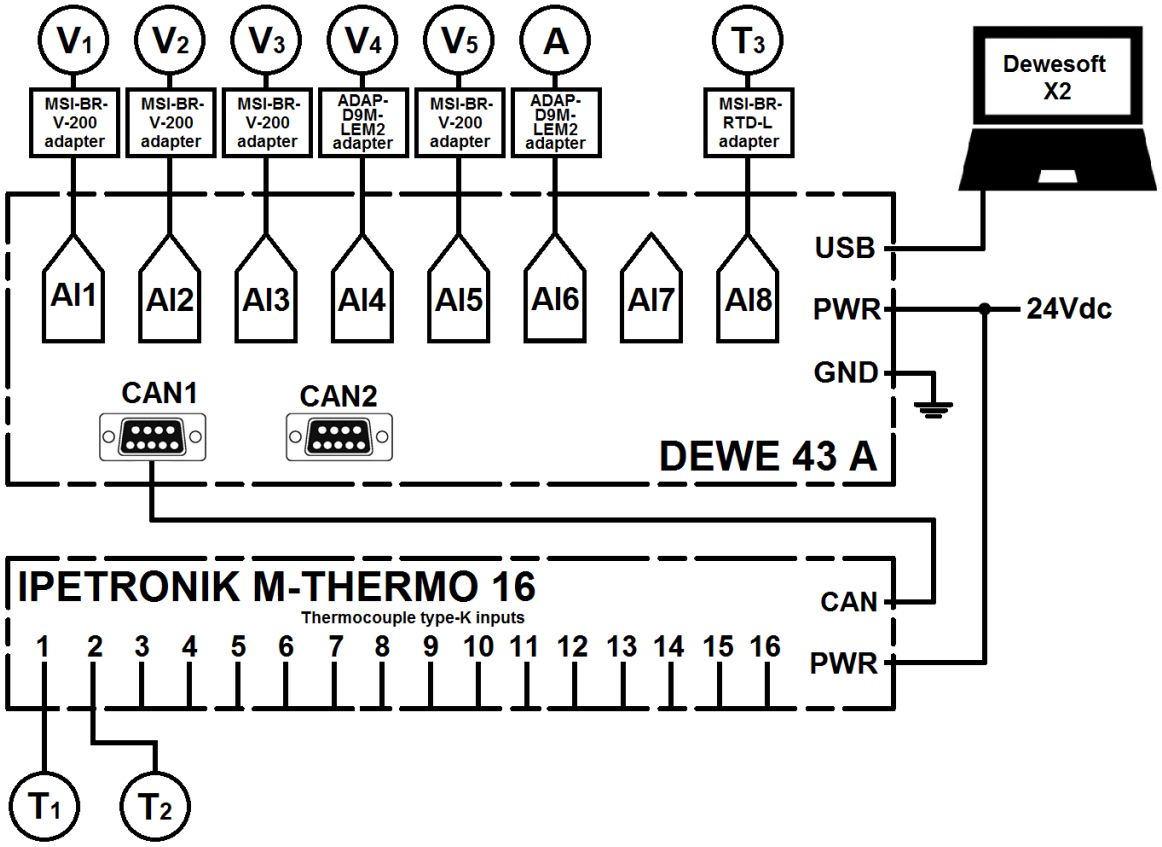

Figure 20. Schematic diagram of the measurement circuit.

The battery temperatures were measured with an external thermocouple measurement device called M-THERMO 16 from the company IPETRONIC. It measured the temperature and sent the data to the DEWE 43 A with CAN bus signals. DEWE 43 A then assembled and placed the data in the file where the other measured values where kept. Figure 20 shows a schematic of how the measurement values were connected to the measurement devices.

Table 2. The sampling rate of the measured signals.

	V1 [S/s]	V2 [S/s]	V3 [S/s]	V4 [S/s]	V5 [S/s]	A [S/s]	T1 [S/s]	T2 [S/s]	T3 [S/s]
Cranking tests	10,000	10,000	10,000	10,000	10,000	10,000	10	10	1
Discharging phase	1	1	-	-	-	1	10	10	1

The sampling rate for the differently measured signals can be seen in table 2 and figure 21 shows a picture of the measurement devices, taken when mounted to the vehicle.

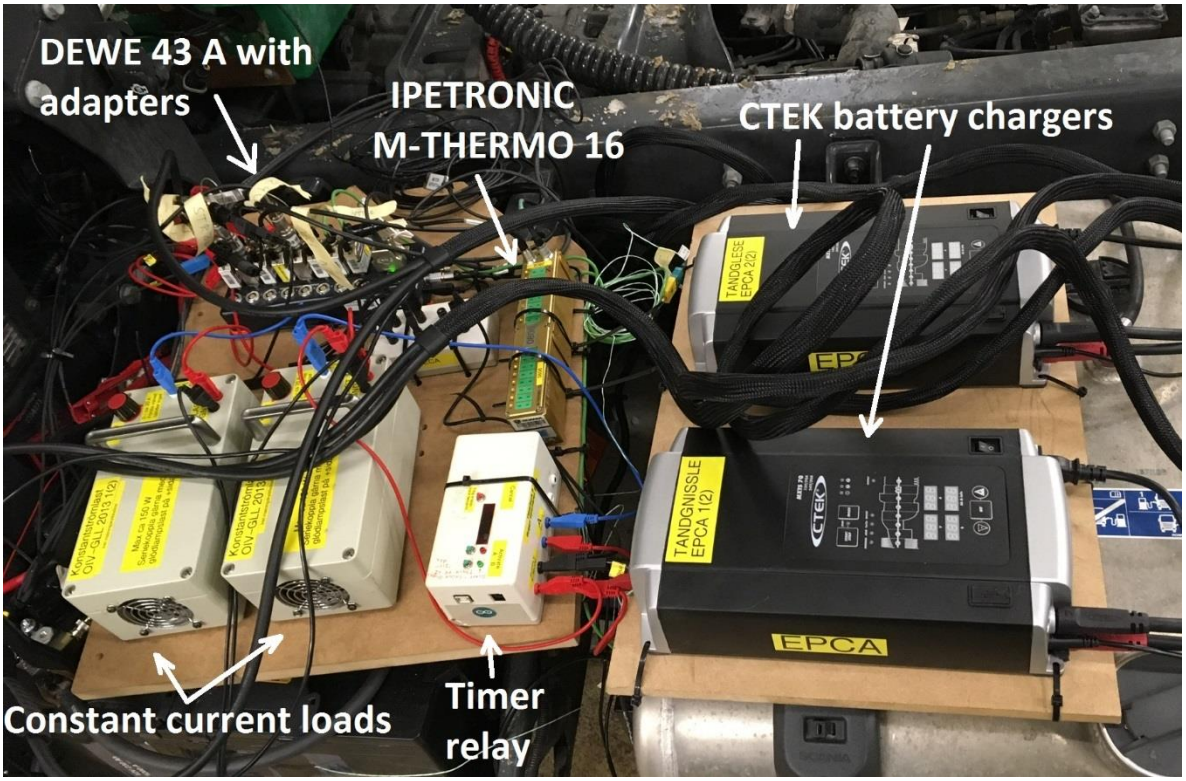

Figure 21. The entire measurement circuit in place and connected along with the battery chargers.

3.4 Analysis of data

DEWEsoft's X2 software was well suited for setting up the DEWE 43 A, but as an analysing tool the X2 proved to be insufficient. The data gathered with the DEWE 43 A during the cranking- and discharging test was therefore converted to .mat files which were loaded into MATLAB and analysed there.

For every cranking- and discharging test a new .mat file with the measured data was saved. This gave many different .mat files for each temperature that was tested. A MATLAB script was written for each temperature, combining the data from these .mat files into variables. Graphs where plotted from the combined data to for the visual analysis of the data for each temperature.

The entire discharging characteristic of each battery voltage and the sum of both batteries voltage, was plotted in one graph for each temperature. The DoD curve was additionally plotted on the same graph, showing how the voltage dropped as the batteries' capacity decreased.

The mean voltage and current between the second and third compression stroke of the engine during cranking was of interest. Then the initial transient conditions, when the starting motor overcame the engines' torque and accelerated the engine's rotation speed, were over. The interval between the second and third compression gave therefore a good idea of batteries' ability to deliver power as the starter motor current consumption was relatively stable. The mean voltage and current of the first and second compression stroke of the engine were measured, if the engine had already begun to rotate independently after the second compression.

MATLAB functions that were available at Scania were used to locate compression strokes 1, 2 and 3 for analysing the recorded data. Other pre-existing functions available at Scania were used to plot a histogram showing the distribution of the 24V voltage during the second and third compression as a function of the batteries' DoD for all starts within each temperature. The same graph additionally showed the main voltage of the second and third compression for each start. A similar histogram was also plotted for the mean current during the same interval for all starts within each temperature.

As the starter motor's current consumption was relatively stable, between the second and third compression stroke, so was its torque, and therefore the rotation speed. The average rotation speed was disproportionate to the product of the time difference between the second and third compression stroke, Δt, and the number of compression strokes for each full revolution of the engine. The vehicle's engine had three compression strokes for each full revolution of the engine, as it was a four stroke, inline 6-cylinder engine. Equation 14 shows how starter motor's average rotation speed, $\dot{n}$, between the two compression strokes was calculated in rpm, revolutions per minute.

$$\dot{n} = \frac{60}{\Delta t \cdot 3} \qquad [14]$$

The last graph plotted for each temperature was of the average rotation speed of the starter motor, between the second and third compression stroke, as a function of the mean voltage for the same interval. This gave a clear picture of the relationship between the starter motor's rotation speed and its input voltage.

4 Results

The startability tests were performed on the following temperatures: +25°C, 0°C, -10°C, -20°C, -25°C, -30°C and -34°C. Due to time limitations, only the gathered data from the temperatures 0°C and -25°C were analysed in this project. The results from the tests during these two temperatures can be seen in the following subchapters.

4.1 The cranking procedure

An understanding of the cranking system's behaviour could be obtained by looking at the vehicle's voltage curve during cranking. A typical voltage curve over both batteries, for the engine used during this project, can be seen in figure 22. The figure was divided into sections for easy explanation of the curve.

Section 1 : Showed the stable voltage when the ignition was on, i.e. feeding all consumers, but did not crank the engine.

Section 2 : Showed the voltage dropping as the ignition was turned to the cranking position. This voltage drop is a result of the meshing solenoid, which meshes the pinion with the ring gear, being magnetized and the starter motor drawing current for holding the armature fixed.

Section 3 : The starter motor drew maximum current from the batteries when the pinion was fully meshed. This high current resulted in a large voltage drop and the starter motor delivering its maximum torque for turning the engine. The torque then increased again with every compression stroke, resulting in a sinusoidal voltage curve.

Section 4 : This section showed the engine beginning to ignite the fuel-air mixture and help the starter motor.

Section 5 : Here, the ignition switch was still in the cranking position but the overrunning clutch had disengaged the armature from the pinion as the engine had begun to turn independently.

Section 6 : Ignitions switch turned off.

Section 7 : This section showed the interval between compression stroke two and three, which was of interest when analysing the data for the histograms as earlier explained in chapter 3.4.

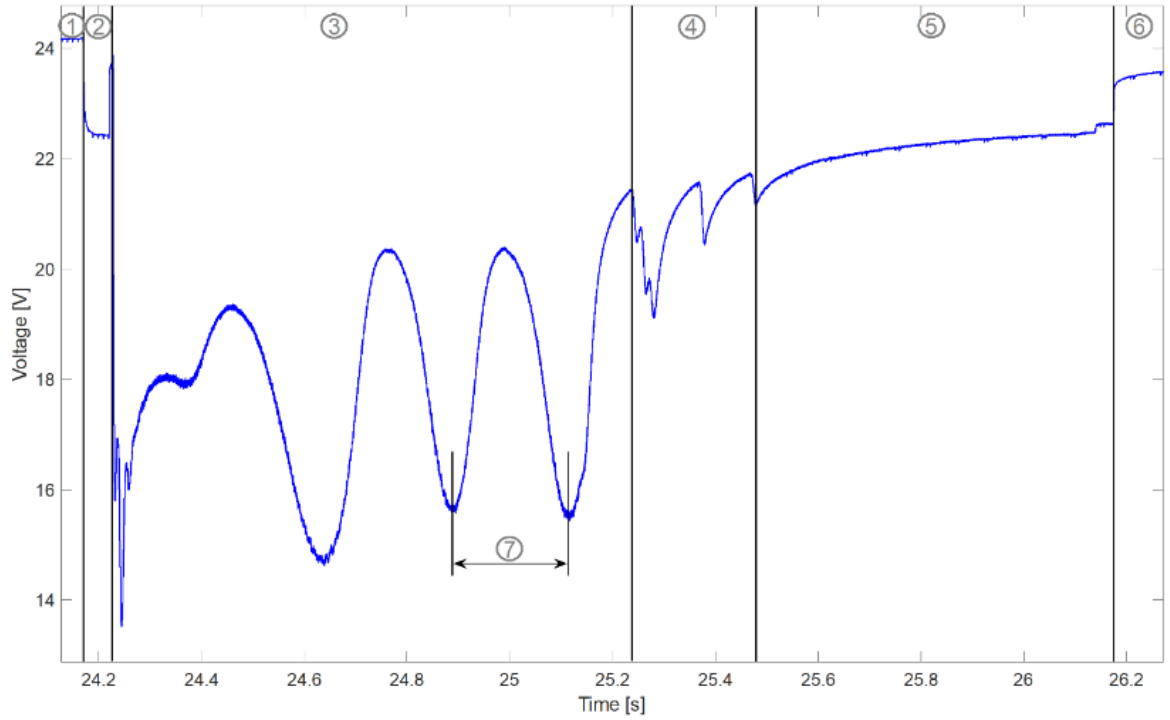

Figure 22. The vehicles voltage curve during cranking.

4.2 Startability test at 0°C

In the ambient temperature 0°C, 13 startability tests were performed. They were performed during a two-day period with no tests during the night. This gave the batteries time to rest during the night and increase the voltage close to OCV. A startability test was therefore performed both at the end of day one and again in the beginning of day two. By doing so, a test was recorded for the voltage the batteries had at the end of day one and the second days' first discharging phase began at a voltage level close to the one the batteries had the night before. Because of this, the first startability test during day two was neglected as it was only used to lower the battery voltage. Therefore, only twelve tests were analysed and plotted for 0°C.

The engine's sump oil had a temperature around -2°C during the startability tests and the batteries between -1.7°C and -0.1°C. The batteries heated up during the discharging procedure.

The discharging phases between each test were plotted one after another in one graph, see figure 23. The green and the magenta curves showed the voltage over the each 12V battery during discharging procedure and the blue curve shows the voltage over both batteries. The peaks off the curves were caused by the batteries' transitions from an unloaded- to a loaded state, that resulted in a voltage drop. In the end of each discharging curve, the voltage increased again when the batteries were disconnected from the discharging loads. The red curve showed the capacity drained from the batteries during the discharging procedure in Ah.

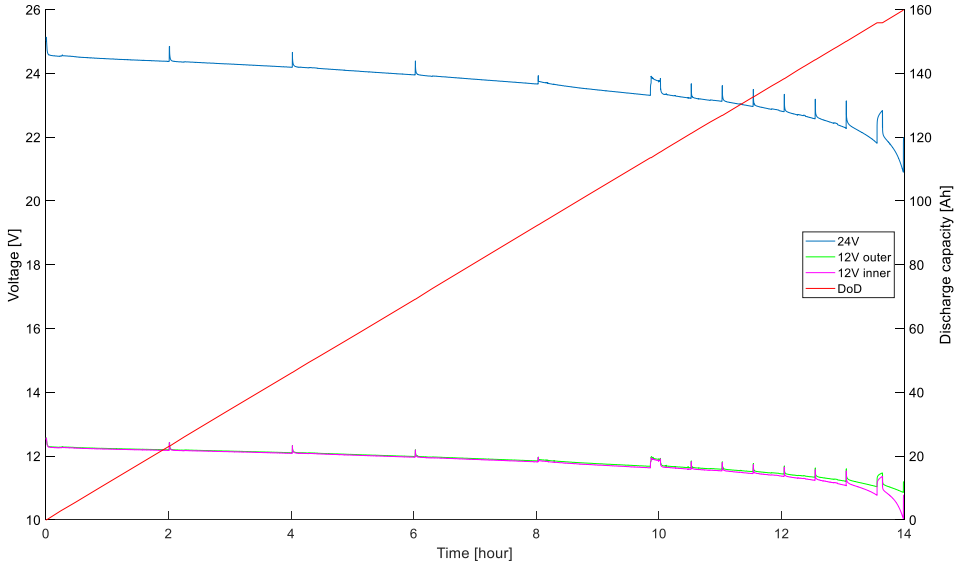

Figure 23. Displays the discharging voltage drop off the batteries and the DoD at 0°C.

Every individual startability test was displayed as a histogram as a function of the DoD that the test was performed at. The histogram represents the sampled data between the second and third compression stroke as described in section 7, figure 22. The width of the histograms represented the number of samples within a limited magnitude interval. Each histogram has a small green square that represents the median value and a small orange dot that was the mean value. A line was plotted trough the mean-value dots to show the mean voltage trend for increasing DoD. The time between each startability test begun with 2 hours (23Ah) until test 6. Thereafter, the intervals were shortened to 30 minutes (5.75 Ah). The histograms for the mean voltage over both batteries can be seen in figure 24 and the mean current in figure 25.

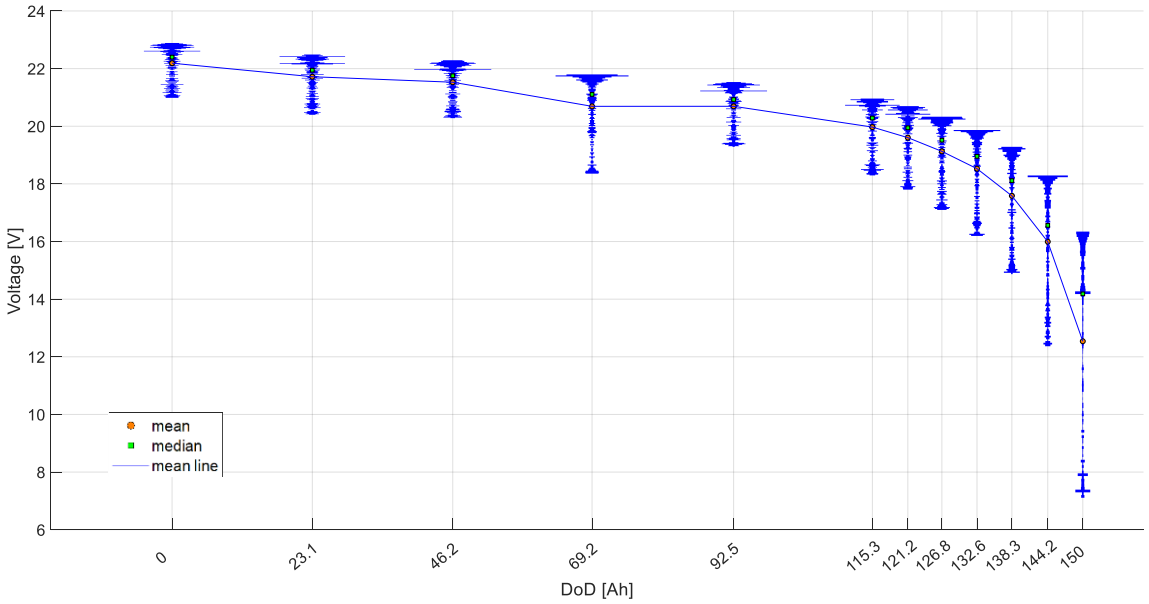

Figure 24. Shows the voltage over both batteries between the second and the third compression stroke during cranking at 0°C. The continuous line follows the mean values.

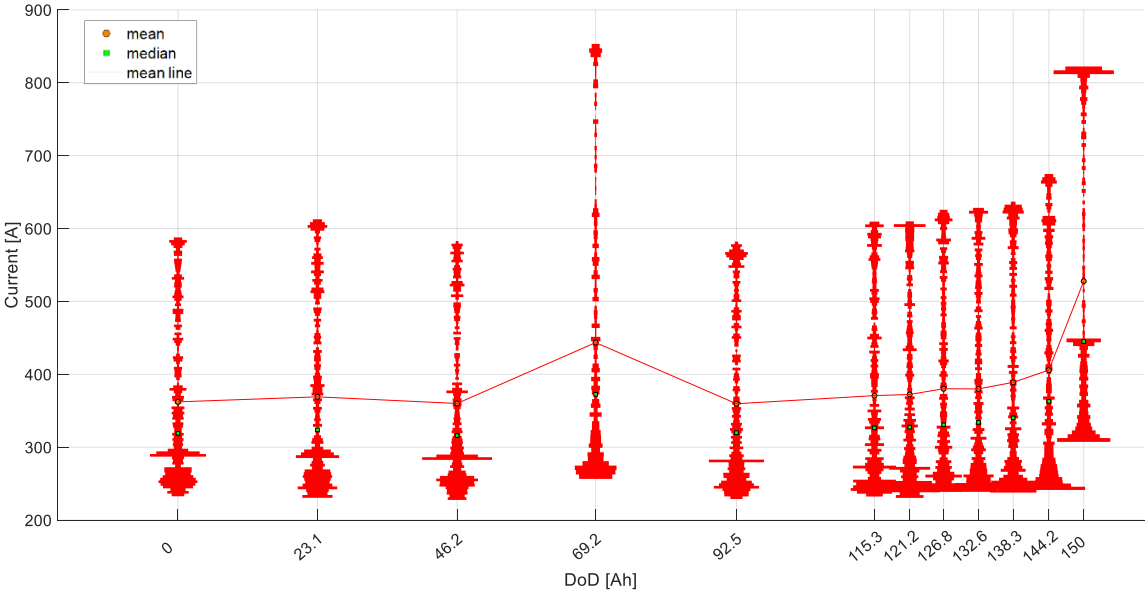

Figure 25. Shows the current through the batteries between the second and the third compression stroke during cranking at 0°C. The continuous line follows the mean values.

The mean voltage for every startability test versus the average rotation speed between the second and the third compression stroke was plotted in figure 26.

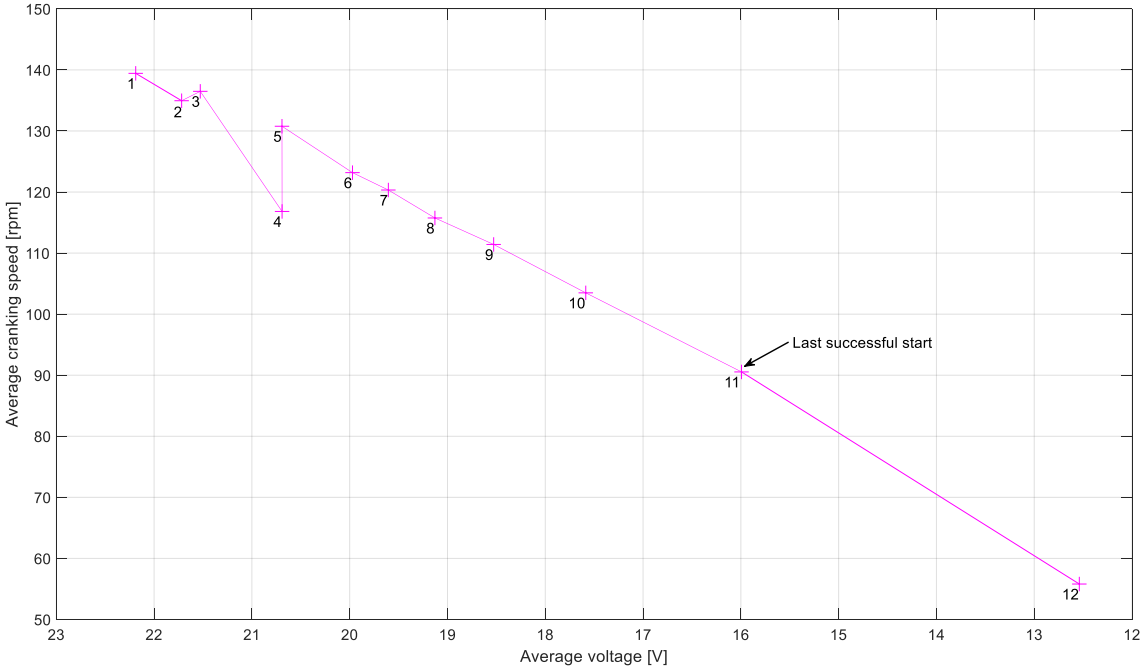

Figure 26. Displays the average cranking speed versus the mean voltage between the second and the third compression stroke at 0°C. The numbers signify which cranking attempt each point represents.

4.3 Startability test at -25°C

At the ambient temperature -25°C, 11 startability tests were performed. All the tests were performed in one day.

The temperature of the engine's sump oil was around -25°C during the tests. The batteries had temperatures that would vary from -24.2°C to -20.4°C, due to the warm up caused by the discharging procedure.

The startability tests and the discharging procedure were plotted in the same way as for the 0°C tests. The time between each test was 30 minutes (5.75 Ah) except between test 1 and 2, 3 and 4 and also between 4 and 5, which had 1 hour (11.5 Ah) between.

The discharging procedure can be seen below in figure 27, the histograms for the cranking mean voltage and current can be seen in figure 28 and figure 29 respectively. Lastly, figure 30 shows the average cranking speed as a function of the mean voltage.

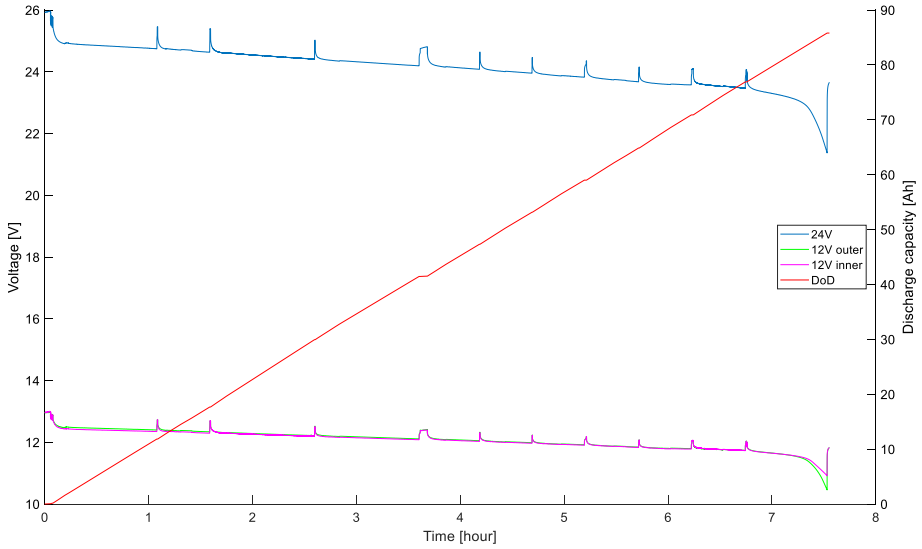

Figure 27. Displays the discharging voltage drop off the batteries and the DoD at -25°C.

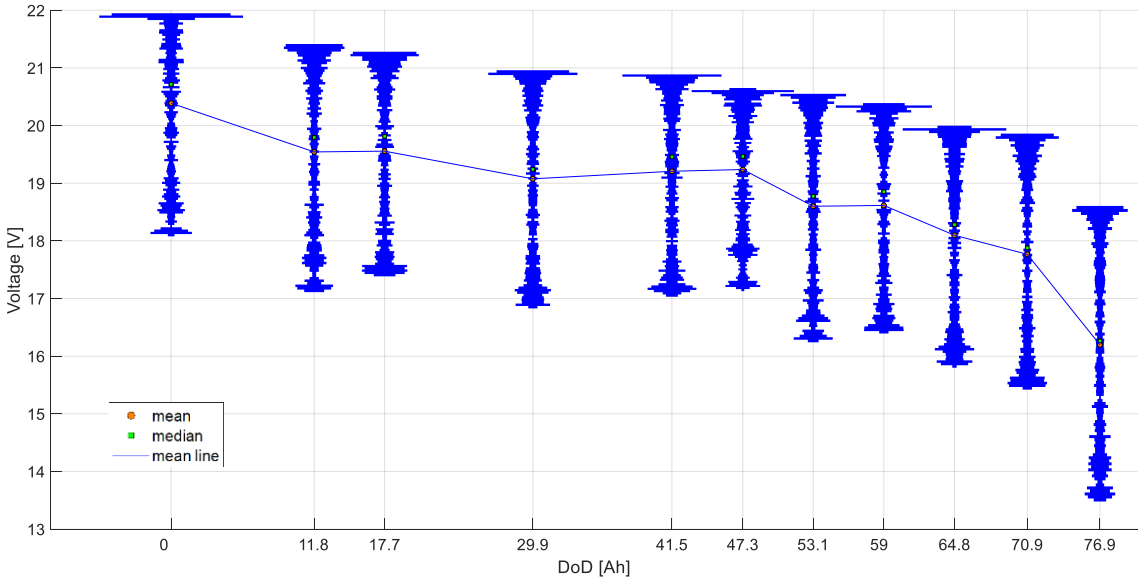

Figure 28. Shows the voltage over both batteries between the second and the third compression stroke during cranking -25°C. The continuous line follows the mean values.

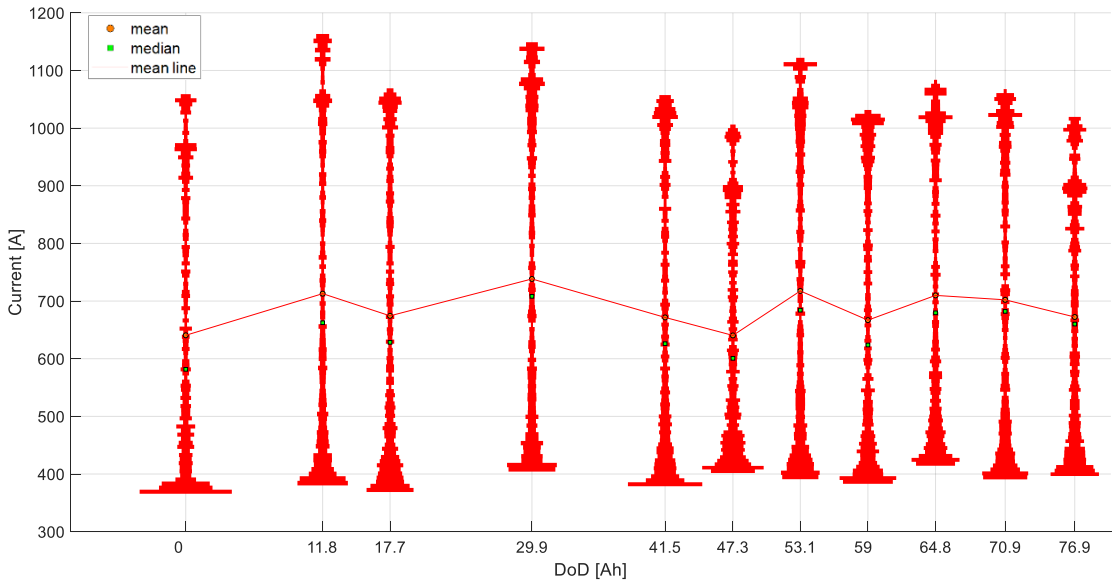

Figure 29. Shows the current through the batteries between the second and the third compression stroke during cranking at -25°C. The continuous line follows the mean values.

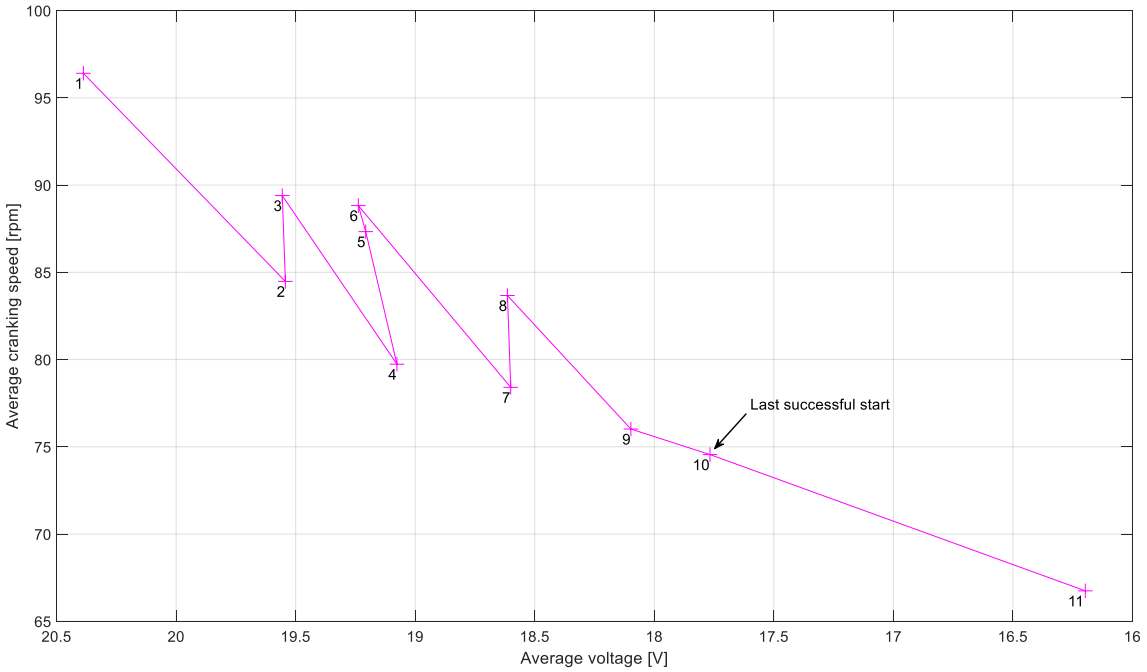

Figure 30. Displays the average cranking speed versus the mean voltage between the second and the third compression stroke at -25°C. The numbers signify which cranking attempt each point represents.

4.4 Battery C20 tests

C20 tests, in accordance with EN 50342-1:2006, were performed before and after the startability tests on each battery that was used. The discharging curves for C20 tests, where the batteries were discharged until they reached deep discharge voltage, can be seen in figures 31 and 32. The data showed that both batteries had lost capacity during the startability tests. The inner battery had 228.1 Ah (100% SoH) capacity at the beginning of the test but after the tests it had 222.2 Ah (97.4% SoH).

The outer battery had 233.3 Ah (100% SoH) capacity at the beginning of the test but after 224.0 Ah (96.0% SoH).

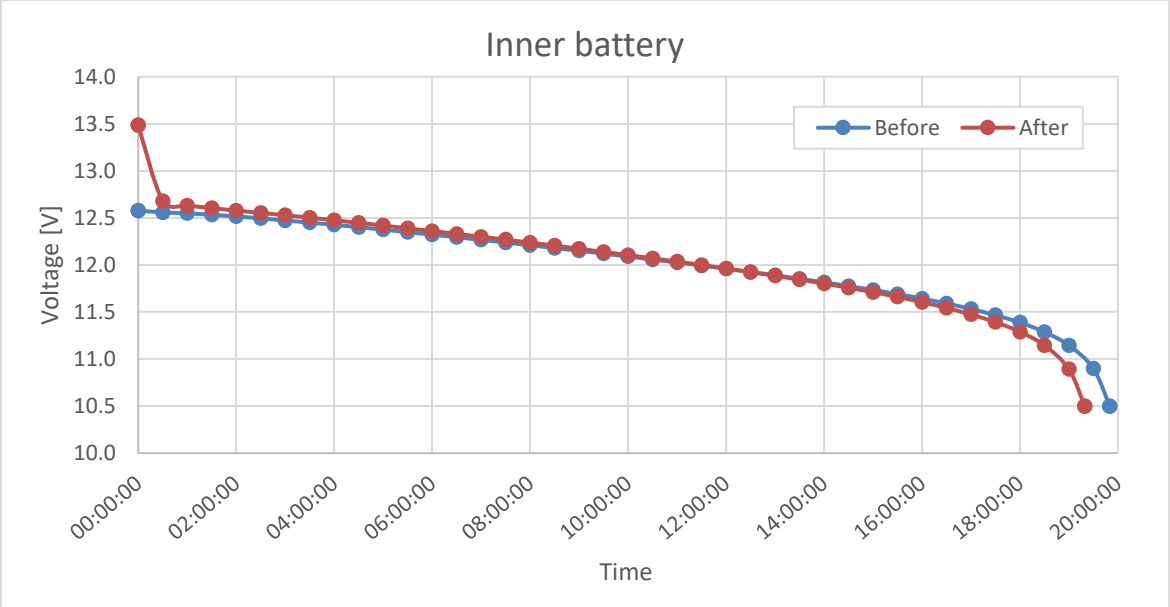

Figure 31. C20 discharging phase of the inner battery.

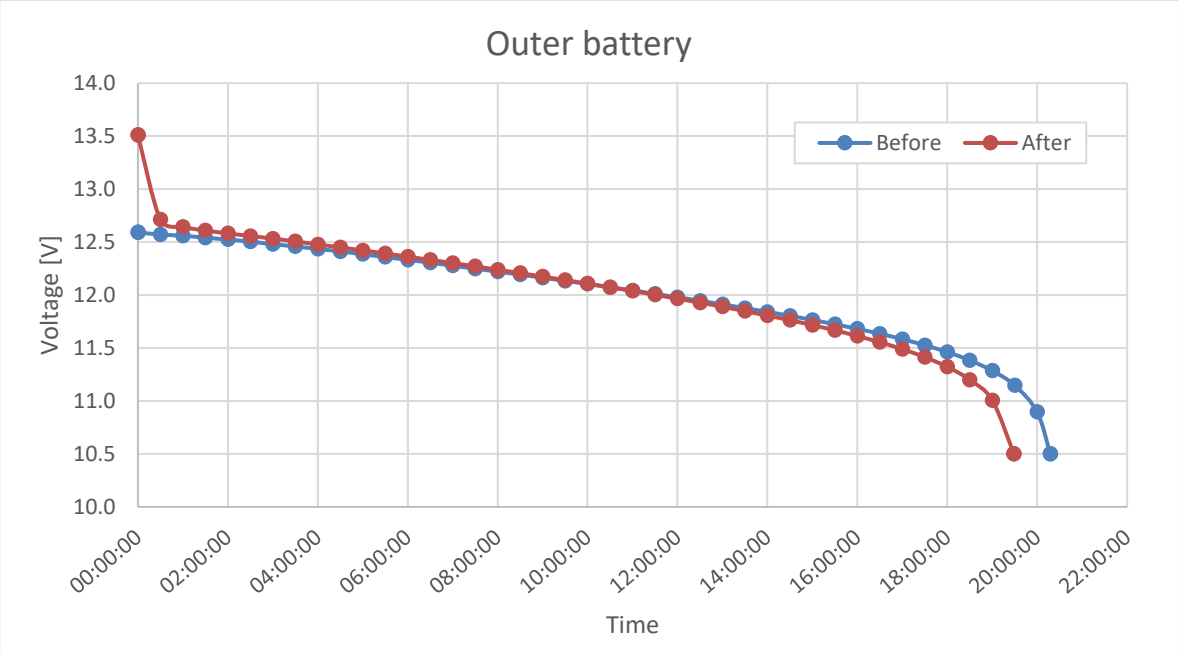

Figure 32. C20 discharging phase of the outer battery.

5 Analysis and discussion

The results of this project show that the goal, to measure the startability of a vehicle in different ambient temperatures and SoC, has been achieved. The startability of a Scania 450hp engine is measured by recording current and voltage in the vehicle's cranking system during cranking at different temperatures. The measurement system performed well for the startability test and delivered reliable data, with a few exceptions at low temperatures. Time limitation made it however only possible to analyse two of the total seven temperatures measured. The analysation was done with MATLAB and showed that the startability of the vehicle decreased with lower battery SoC and that the batteries are faster to reached lower SoC at lower temperatures.

5.1 Analysis of the measurement method

The measurement method used to measure the vehicle's startability gave reliant and accurate measurement data. The analogue shunt resistor ammeter that was used could have been calibrated in the DEWEsoft's setup software, X2. But the shunts known resistance (0.1mΩ), which gave a 10,000A for every 1V voltage drop, was used as no calibration instruments were available at Scania to calibrate at the high currents needed. The analogue shunt resistor was however compared to a calibrated digital shunt which showed that the analogue shunt was sufficiently accurate at high currents and could be sampled at the desired rate.

Both of the earlier mentioned voltage measurement methods were used as they showed little difference when compared. Method 1 (one coaxial cable) gave a 10mV lower voltage reading than method 2 (two coaxial cables) which could be caused by a small resistance difference between the cables used. No noticeable noise difference was observed between the methods. It was therefore evaluated to have no effect on the measurement results to use both methods.

Other measurement devices available at Scania, such as analogue Isabellehütte current shunts connected to a CANcase, could have been used. They were however ruled out as their maximum sampling rate was insufficient to attain the cranking systems fastest transients. The sampling rate that was used for measuring the voltage and current during the startability tests (10 kS/s) was nevertheless higher than actually needed to gather the desired data. This sampling rate however made it possible to detect fast transients in the measured signals with higher precision. Other signals were measured at the lowest available sampling rate as they had a slow rate of change.

Nine analogue measurements were required by the measurement method. This introduces a problem as the DEWE 43 A only has eight analogue inputs. This was solved by measuring the battery temperature with another measurement devise, the IPETRONIK M-THERMO 16, which then sent the measured data to the DEWE 43 A via CAN-signals. It was originally planned to use thermocouple sensors for all temperature measurements. But a PT100 temperature sensor was used for

measuring the oil sump temperature as it was already mounted to the vehicle sump and could easily be measured with the help of an adapter.

The measurement circuit worked, as earlier stated, very well for measuring the vehicles startability. However, some adjustments had to be made at low temperatures as some of the measurement circuits electronical devices stopped working. For temperatures lower than -20°C the DEWE 43 A and the IPETRONIK M-THERMO 16 stopped working. This was unfortunate as startability tests had been planned at several temperatures lower than -20°C. This was resolved by wrapping the DEWE and M-THERMO 16 in a 50W heating mat and insulating it from the ambient temperature by placing them inside cardboard box. Figure 33 shows a photo of the DEWE and M-THERMO in the cardboard box. The timer relay did also not work at those extreme sub-zero temperatures but that problem was resolved by manually controlling the discharging phase with the help of a stopwatch.

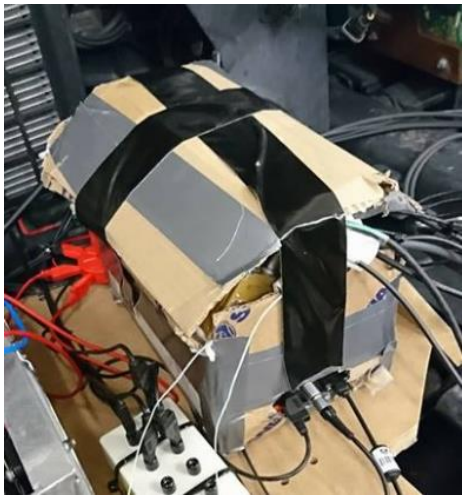

Figure 33. The measurement devices' wrapped in carboard box and heating mat for sub-zero temperature operations.

Some problems, like the ones previously explained, were expected at the extreme temperatures. The vehicle was therefore refuelled with winter diesel before the startability testing begun to eliminate the risk of it not starting because of paraffin build up in the fuel system. Paraffin did however build up in the fuel system at the lowest measured temperature as some normal diesel was left in the vehicle's fuel filters after refuelling. The engine's fuel filters, therefore, had to be changed and the summer diesel washed out from the fuels system by allowing the engine to run until it reached operating temperature.

Many different signals were measured during the startability testing, resulting in a large amount of gathered data. MATLAB was used to analyse the data as it is practical and easy to analyse large quantities of data with it. A function was made for each temperature that gathered all the measured data into MATLAB scripts. Other functions, pre-existing at Scania, were also used to analyse and plot graphs showing the results of the tests. The projects timeframe only allowed for analysing of two tested temperatures out of the seven measured as the measurement phase was more demanding and time consuming the was expected. These two temperatures give

however a good understanding of the vehicles startability. A more comprehensive analysis of the results can be seen in chapter 5.2

The measurement circuit and devices used gave clear results that could be used to analyse the vehicles startability. Other systems, then the cranking system, however have effect on the vehicles ability to start. It is therefore recommended, for future research on startability, to measure the engine's torque and rpm along with gathering the engine's control computers signals, to get a deeper understanding of the entire system. Additionally, it is recommended to evaluate what effect extreme temperatures can have on the vehicle and the measurement circuit before testing begins.

5.2 Analysis of the results

At the ambient temperature 0°C, a total capacity of 159.8 Ah was discharged until the inner battery reached the deep-discharged voltage. That capacity was quite close to the average capacity of 166 Ah, for C20 current, at 0°C given by the manufacturer, see table 1 in chapter 2.2.1.3. This difference may be a result of the manufacturer's stable testing conditions, compared to the slightly variating temperature of the batteries (-1.7°C to -0.1°C) during this project's discharging procedure. The constant current loads did also vary with the batteries voltage, which required manual adjustments to keep a constant current during the discharging phase. Yet another factor that may have had an impact on the discharged capacity were the 13 performed startability tests. During these tests, the cranking procedure's average discharging current was approximative 400 A but only for a period shorter than 2 seconds. According to the Peukert's law, the batteries' total delivered capacity will decrease when the current increases. Hence the high cranking current may have affected the total capacity even though it only lasted for a few seconds.

The total discharged capacity during the temperature -25°C was 85.9 Ah until the outer battery dropped to deep-discharge voltage. There was no data from the manufacturer of the capacity at -25°C to compare the discharged capacity with. But according to table 1 in chapter 2.2.1.3, an approximative linear trend can be found. The trend gives an estimated capacity of 100 Ah at -25°C, which is higher than the discharged capacity of 85.9 Ah. This capacity difference, similarly to the difference at 0°C, could be a result of the higher average cranking current at -25°C, that was around 700 A compared to 400 A at 0°C. The higher cranking current would according to the Peukert's law, decrease the capacity more during each cranking performance at -25°C than at 0°C. The cranking procedure lasted also around 1 second longer at -25°C than at 0°C which may also affect the capacity. To predict the capacity at -25°C with more accuracy, further C20 battery tests at temperatures below -20°C must be performed.

The inner battery dropped first to deep-discharge voltage at 0°C, during the last discharging phase after the startability tests were done. At -25°C as an opposite happened, the outer battery reached deep-discharged voltage before the inner battery. The same trend was observed during testing at -20°C and +25°C. The inner battery therefore dropped before the outer at the warmer temperature and in reverse order at the cooler temperature. The inner battery lasted for a shorter time than the

outer during the C20 at +25°C tests before and after the startability tests. Hence, the trend showed that the inner battery performed worse than the outer when discharged with a C20 current at temperatures above 0°C. On the other hand, in sub-zero temperatures, the outer battery performed worse when discharged with a C20 discharging current. This inverse behaviour could be a result of the outer battery being more difficult to discharge at sub-zero temperatures than the inner battery.

The average voltages during the cranking procedure at 0°C shows that the mean voltage decreased at a faster rate after the sixth startability test, as can be seen in figure 24. The mean voltage curve had a concave form similar to the discharging curve in figure 23. Both of these curves declined faster closer to the end. The same curves for -25°C also showed a concave form but declined at an even faster rate in the end. This could be an effect of the batteries performing worse at cooler temperatures.

Figure 26 and 30 show graphs of the engine's average rotation speed during cranking as a function of the cranking systems average voltage for temperatures 0°C and -25°C, respectively. The graphs show that the rotation speed of the starter motor decreases with the voltage, as per the series-wound DC motors theory. The graphs also show that the rotation speed and the average voltage during cranking has a relatively linear trend. It can also be seen by taking the average current histograms (figure 25 and 29) into account, that the required current to reach a specific rotation speed increases and the voltage drops with lowering temperature. This supports the theory that the powertrain torque increases with decreasing temperatures.

All the behaviours described above, are of importance to predict startability. This is shown by the mean voltage during the cranking procedure for 0°C and -25°C. The last successfully start at -25°C had a mean voltage of 17.8 V and an average rotation speed of 74.5 rpm, meanwhile it was only 16 V with the rotation speed of 90.5 rpm at 0°C. The last cranking procedure at -25°C couldn't start the engine at the reached rotation speed of 66.7 rpm. Hence the rotation speed for startability is between 74.5 and 66.7 rpm at -25°C. The last cranking at 0°C resulted in a rotation speed of 55.8 rpm, hence the startability at 0°C lies between 90.5 and 55.8 rpm.

The average voltage curve for several temperatures must be examined and compared with the discharging curve for the same temperature, to predict the vehicles startability. The increasing drag torque of the powertrain at lower temperatures along with the batteries decreasing performance, makes the startability hard to predict without gathering test data. The C20 tests before and after the startability tests show that it can be difficult to predict the vehicles startability even though the data is attained, as the batteries age and deteriorate with time and increasing number of cranks.

5.3 Applications and advantages with the understanding of startability

An understanding of the startability is of importance to optimize the life time of the lead-acid batteries in commercial vehicles. The effect that many cranking procedures along with deep discharges have on the batteries is critical when predicting their life

time. With a good understanding of startability, the batteries life time can be increased by avoiding harmful battery conditions such as deep discharging.

In modern vehicles, start and stop applications are becoming more common to save fuel. For these applications, the startability is a central topic. The negative impact of bad startability knowledge, resulting in frequent vehicle battery replacement, could outweigh the environmental and economic benefits gained in fuel saving, with the start and stop application. Another advantage of understanding the startability of a diesel fuelled commercial vehicle, is for comparison and benchmarking with engines that are fuelled with non-fossil propellants. This is important when deciding if to introduce non-fossil propellants in temperate countries with cold winters.

An economical aspect while operating a commercial vehicle, is to reduce the unwanted downtime i.e. VOR, vehicle off road. VOR can be very costly for the vehicle since the vehicle doesn't generate any income during its downtime. VOR caused by the cranking systems inability to start the engine due to excessive drained batteries can be avoided with good startability knowledge. Another, environmental, aspect with good startability knowledge is to avoid deep discharging of the batteries. By avoiding deep discharge, the life time of the batteries can be increased so they don't have to be replaced as frequently. This reduction in battery replacement, will consequently decrease the need for production and recycling of the battery's hazardous materials. Which will lower the total impact that vehicle batteries have on the environment.

6 Conclusion

A knowledge of a vehicle's startability is important to reliably predict when the vehicle battery capacity has reached the point where reliable engine starting is threatened. In this project, startability tests were planned and performed on a Scania long haulage truck, with a 450hp engine, at different temperatures and battery SoC. Two of these temperatures; 0°C and -25°C, were analysed with MATLAB.

The results of these tests show that the powertrain's torque increases with lower temperatures while the batteries performance decreases. This results in a worse startability at -25°C then at 0°C. At 0°C the cranking system could crank the engine to turnover speed until 144.2 Ah had been drained from the batteries while at -25°C the vehicles last successful crank was at 70.9 Ah battery discharge. This difference is a result of the vehicle's cranking system requiring higher current and higher voltage for the engine to reach turnover speed at lower temperatures. The higher current required is due to the increase in engine torque while the higher voltage is due to the battery worse performance at lower temperatures. One battery performed better at warmer temperatures but then performed worse at sub-zero temperatures compared to the other battery. The results also show that the vehicle's batteries SoH decreased to 97.4% and 96.0% of capacity they had before testing began.

Certain factors are important to keep in mind before performing a startability test at sub-zero temperatures. One is to refuel the vehicle with winter diesel and change fuel filters before performing the tests at extreme sub-zero temperatures. This is to prevent paraffin building up in the fuel system. Another is to heat the measuring instruments as they may stop working properly at extreme sub-zero temperatures.

New fuel saving applications and an increasing number of electrical consumers in modern commercial vehicles have made the startability of large importance. Both to increase the batteries' lifetime and for a more reliable cranking. For better understanding of the vehicle's startability, further testing with batteries at different stages in their lifecycle and diverse temperatures is recommended.

Bibliography

1. Robert Bosch GmbH. Automotive electrics Automotive Electronics. 5th ed. West Sussex: John Wiley & Sons Ltd.; 2007.

2. Robert Bosch GmbH. Alternators and starter motors. 1st ed. Horst B, editor. Plochingen: Robert Bosch GmbH; 2003.

3. Cameron, G. L.; Pettit, C. W.; Rowls, G. A.. Cold Cranking Team: Battery, Cables, Cranking Motor, Engine Oil. In Zhou Y. The Role of Engine Oil Viscosity in Low Temperature Cranking and Starting. Saint Louis: Elsevier Sience; 1966. p. 9-20.

4. Cugnet M, Sabatier J, Laruelle S, Grugeon S, Sahut B, Oustaloup A, et al. On Lead-Acid-Battery Resistance and Cranking-Capability Estimation. IEEE Transations on Industrial Electronics. 2010 March; 57(3).

5. Crolla D, Mashadi B. Vehicle Powertrain Systems Chichester: John Wiley & Sons Inc.; 2012.

6. Robert Bosch GmdH. Automtovie Handbook. 8th ed. Plochingen: Jhon Wiley & Sons Ltd.; 2011.

7. Swedish powertrain. [Online].; 2018 [cited 2018 April 19 [Image]. Available from: http://www.swedishpowertrain.com/en/products.html.

8. Harald N, Bernd B, Joachim R, Wolfgang N. Automotive transmissions Fundamentals, Selection, Design and Application. 2nd ed. Berlin: Springer-Verlag Berlin Heidelberg; 2011.

9. Exide. www.tudor.se. [Online].; 2009 [cited 2018 03 28. Available from: http://tudor.se/startbatteriets-konstruktion-och-funktion/.

10. Exide. www.tudor.se. [Online].; 2013 [cited 2018 03 28. Available from: http://tudor.se/fokus-pa-blybatterier-2/.

11. Europe ET. Lead Acid Battery Presentation. 2014. A conference presentation.

12. Peters K. Design options for automotive batteries in advanced car electrical. Teknisk rapport. Manchester: Journal of Power Sources, Battery Design and Manufacturing Systems; 1999.

13. Eberhard Meissner GR. Battery Monitoring and Electrical Energy Management. Journal of Power Sources. 2003; 116(1-2).

14. Dennis Doerffel SAS. A critical review of using the Peukert equation for determining the remaining capacity of lead-acid and lithium-ion batteries. Journal of Power Sources. 2005 April; 155(2).

15. Hausmann A, Depcik C. Expanding the Peukert equation for battery capacity modeling through inclusion. Journal of Power Sources. 2013 Feb; 235(1).

16. Svensson C. www.tudor.se. [Online].; 2009 [cited 2018 05 11. Available from: http://tudor.se/ny-bilteknik-forandrar-kraven-pa-batterierna/.

17. Exide technologies. Battery management - From battery reception to truck sales. April 2011. Powerpoint persentation.

18. Svensson C. www.tudor.se. [Online].; 2010 [cited 2018 05 11. Available from: http://tudor.se/laddning-av-batterier/.

19. Franzén T, Lundgren S. Elkraftteknik. 1st ed. Malmö: Holmbergs i Malmö AB; 2013.

20. Forouzan B. Data Communications and Networking. 5th ed. New York: McGraw-Hill; 2012.

21. Schon K. High Impulse Voltage and Current Measurement Techniques. 1st ed. Berlin: Springer; 2013.

22. Boylestad LR. Introductory Circuit Analysis. 13th ed. Gilffillan A, editor. Essex: Pearson Education Limited; 2016.

23. Williams J. Thermocouple measuerement. In Dobkin B, Williams J. Analog Circuit Design - A Tutorial Guide to Applications and Solutions. Oxford: Elsevier Inc.; 2011. p. 596-613.

24. Ibrahim D. Microcontroller-Based Temperature Monitoring and Control. 1st ed. Oxford: Newnes; 2002.

25. Isabellenhütte Heusler GmbH & Co. KG. MANGANIN. [Online].; 2014 [cited 2017 May 17 [Data sheet from Isabellenhütte]. Available from: https://www.isabellenhuette.de/fileadmin/Daten/Praezisionslegierungen/Datenblaetter_Widerstand/Englisch/MANGANIN.pdf.

26. Dellinger JH. National Institute of Standards and Technology. [Online].; 1910 [cited 2018 May 17. Available from: https://nvlpubs.nist.gov/nistpubs/bulletin/07/nbsbulletinv7n1p71_A2b.pdf.

27. DEWEsoft. [Online]. [cited 2018 May 18. Available from: https://www.dewesoft.com/products/dewe-43.

28. Eriksson L, Nielsen L. Modelling and control of engines and drivelines. 1st ed. Chichester: John Wiley & Sons Ltd; 2014.

29. Anette, Myhr. Fordon 2017 - Statistik 2018:05. [Online]. Stockholm; 2018 [cited 2018 April 4. Available from: https://www.trafa.se/globalassets/statistik/vagtrafik/fordon/2018/fordon_2017_blad.pdf?

30. Michalski L, Eckersdorf K, Kurcharski J, McGhee J. Temperature Mesasurement. 2nd ed. Chichester: John Wiley & Sons Ltd.; 2001.

31. Hausmann A, Depcik C. Expanding the Peukert equation for battery capacity modeling through inclusion. Journal of Power Sources. 2013 Feb; 235(1).

32. Doerffel D, Sharkh SA. A critical review of using the Peukert equation for determining the remaining capacity of lead-acid and lithium-ion batteries. Journal of Power Sources. 2005 April; 155(2).

33. Meissner E, Richter G. Battery Monitoring and Electrical Energy Management. Journal of Power Sources. 2003; 116(1-2).

34. Svensson, Christer. www.tudor.se. [Online].; 2010 [cited 2018 05 11. Available from: http://tudor.se/laddning-av-batterier/.

TRITA CBH-GRU-2018:51